# Future climatic drivers and their effect on PM10 components in Europe and the Mediterranean Sea

Arineh Cholakian, Augustin Colette, Isabelle Coll, Giancarlo Ciarelli, Matthias Beekmann

Atmos. Chem. Phys., 19, 4459–4484, 2019
https://doi.org/10.5194/acp-19-4459-2019


Atmospheric Chemistry and Physics
Open Access
EGU

# Future climatic drivers and their effect on $PM_{10}$ components in Europe and the Mediterranean Sea

**Arineh Cholakian**[1,2,a], **Augustin Colette**[2], **Isabelle Coll**[1], **Giancarlo Ciarelli**[1,b], **and Matthias Beekmann**[1]

[1]Laboratoire Interuniversitaire des Systèmes Atmosphériques (LISA), UMR CNRS 7583,
Université Paris Est Créteil et Université Paris Diderot (UPD), Institut Pierre Simon Laplace, Créteil (IPSL), Créteil, France
[2]Institut National de l'Environnement Industriel et des Risques, Parc Technologique ALATA, Verneuil-en-Halatte, France
[a]now at: EPOC, UMR 5805, Université de Bordeaux, Pessac, France
[b]now at: Department of Chemical Engineering, Carnegie Mellon University, Pittsburgh, USA

**Correspondence:** Arineh Cholakian (arineh.cholakian@lisa.u-pec.fr)

Received: 21 August 2018 – Discussion started: 5 December 2018
Revised: 26 February 2019 – Accepted: 18 March 2019 – Published: 5 April 2019

**Abstract.** Multiple CMIP5 (Coupled Model Intercomparison Project phase 5) future scenarios run with the CHIMERE chemistry transport model (CTM) are compared to historic simulations in order to study some of the drivers governing air pollution. Here, the focus is on regional climate, anthropogenic emissions and long-range transport. Two major subdomains are explored – the European region and the Mediterranean Basin – with both areas showing high sensitivity to climate change. The Mediterranean area is explored in the context of the ChArMEx (the Chemistry Aerosol Mediterranean Experiment) project, which examines the current and future meteorological and chemical conditions of the Mediterranean area. This climate impact study covers the period from 2031 to 2100 and considers possible future scenarios in comparison with 1976 to 2005 historic simulations using three Representative Concentration Pathways (RCPs; RCP2.6, RCP4.5 and RCP8.5). A detailed analysis of total $PM_{10}$ (particulate matter with a diameter smaller that 10 µm) concentrations is carried out, including the evolution of $PM_{10}$ and changes to its composition. The individual effects of meteorological conditions on $PM_{10}$ components are explored in these scenarios in an effort to pinpoint the meteorological parameter(s) governing each component. The anthropogenic emission impact study covers the period from 2046 to 2055 using current legislation (CLE) and maximum feasible reduction (MFR) anthropogenic emissions for the year 2050 compared with historic simulations covering the period from 1996 to 2005 and utilizing CLE2010 emissions data. Long-range transport is explored by changing the boundary conditions in the chemistry transport model over the same period as the emission impact studies. Finally, a cumulative effect analysis of these drivers is performed, and the impact of each driver on $PM_{10}$ and its components is estimated. The results show that regional climate change causes a decrease in the $PM_{10}$ concentrations in our scenarios (in both the European and Mediterranean subdomains), as a result of a decrease in nitrate, sulfate, ammonium and dust atmospheric concentrations in most scenarios. On the contrary, BSOA (biogenic secondary organic aerosol) displays an important increase in all scenarios, showing more pronounced concentrations for the European subdomain compared with the Mediterranean region. Regarding the relationship of different meteorological parameters to concentrations of different species, nitrate and BSOA show a strong temperature dependence, whereas sulfate is most strongly correlated with relative humidity. The temperature-dependent behavior of BSOA changes when looking at the Mediterranean subdomain, where it displays more dependence on wind speed, due to the transported nature of BSOA existing in this subdomain. A cumulative look at all drivers shows that anthropogenic emission changes overshadow changes caused by climate and long-range transport for both of the subdomains explored, with the exception of dust particles for which long-range transport changes are more influential, especially in the Mediterranean Basin. For certain species (such as sulfates and BSOA), in most of the subdomains explored, the changes caused by anthropogenic emissions are (to a certain

extent) reduced by the boundary conditions and regional climate changes.

## 1 Introduction

Particulate matter (PM) is one of the most important constituents of air pollution. It can have a variety of adverse effects on air quality (Seinfeld and Pandis, 2016) and, subsequently, on human health (Pope and Dockery, 2006; Kampa and Castanas, 2008; Anderson et al., 2012; Im et al., 2018) and ecosystems (Grantz et al., 2003). Studies have shown that the life expectancy of the population can change drastically in areas densely polluted by atmospheric aerosols (Pope et al., 2009). PM is comprised of a large number of components, with different origins and diverse behaviors with respect to meteorological parameters. Therefore, there are many different ways in which the particles can affect air quality, making their investigation both important and complex.

The intricacy of studying PM increases when coupling its effects with climate change, as air quality and climate change have intertwined interactions (e.g., Kinney, 2008; Wild, 2009; Seinfeld and Pandis, 2016). In other words, changes in meteorological conditions have varied effects on air quality, but at the same time climate change may be affected by the radiative forcing of air pollutants. These effects can, in some cases, be similar in direction, or they may cause inverse outcomes. Thus, when exploring future air quality, it is important to take into account that different drivers can have different impacts while also undergoing nonlinear interactions among themselves. Therefore it is necessary to explore the effects of each driver separately.

Air pollution is mainly governed by four factors: anthropogenic and/or biogenic emissions of primary pollutants and precursors of secondary pollutants, atmospheric chemistry, long-range transport and, of course, meteorology (Jacob and Winner, 2009). While these factors are listed separately, they also undergo interactions among themselves. For example, atmospheric chemistry is directly affected by temperature and radiative forcing. Similarly, parameters such as precipitation, wind speed and wind direction can enhance or reduce dispersion and deposition. Furthermore, meteorological conditions such as temperature and wind speed can indirectly impact the emission of primary pollutants, which may also be precursors of secondary pollutants (EEA, 2004). As a result, the sensitivity of air quality to climate change seems to be crucial, but complex to investigate.

The sensitivity of different areas in the world to climate change depends on the existing local meteorological conditions. Giorgi (2006) calculated a factor to determine climate change hotspots in future scenarios and to establish the sensitivity of different regions when faced with climate change. Using the differences between historic and future precipitation and temperature for different regions and seasons in an ensemble of scenarios and models, he showed that the Mediterranean and northeastern European regions are more sensitive to climate change than other areas of the world, followed by the western Europe. According to his calculations, the European region (both the eastern and western regions on average) and the Mediterranean as a whole, are among the most important hotspots for climate change. This highlights the importance of understanding changes that might affect these regions. Therefore, the focus of this study is on the European area with special attention paid to the Mediterranean Basin, which is why the current work is related to the ChArMEx (the Chemistry Aerosol Mediterranean Experiment; http://charmex.lsce.ipsl.fr, last access: 7 September 2018) project. The goals of ChArMEx are to better assess the sources, formation, transformation and mechanisms of transportation of gases and aerosols in the western Mediterranean Basin and also to better estimate the future composition of the atmosphere over the Mediterranean Sea. The measurement portion of this campaign took place in the western Mediterranean Basin during the period from 2012 to 2014; however, the analysis of the data obtained during the campaign and the assessment of future atmospheric changes for the basin are still ongoing.

A regional chemistry transport model (CTM) was used to explore possible future changes in these regions. Running such regional simulations requires inputs from a global CTM, a global circulation model (GCM) and a regional climate model (RCM), as well as anthropogenic/biogenic emission inputs. Changes made to these inputs make it possible to distinguish the effects of different drivers on air pollution one by one. Modifying RCM inputs allows for the estimation of the effects of meteorology alone, whereas a combined modification of RCM and global CTM inputs allows for the simultaneous assessment of the impacts of meteorology and long-range transport. Conversely, apart from RCM inputs, changes in anthropogenic emissions allow for the exploration of the effects of meteorology and emissions on air pollution.

These kinds of studies naturally already exist for different parts of the world, for one or multiple drivers and for different components. For example, Liao et al. (2006) used a global model to explore the atmospheric changes expected in the year 2100; this was undertaken by comparing a year of historic simulations with a yearlong simulation in 2100, where all factors were changed. The first study that investigated the future atmospheric conditions of a European area only focused on ozone changes and used the two 30-year-long future scenarios compared with a 30-year-long historic period (Meleux et al., 2007). Other studies have used an ensemble of future simulations, each with a different model, in order to compare the results given by each of these models (e.g., Langner et al., 2012). Based on the IMPACT2C project (Jacob, 2017), Lacressonnière et al. (2016, 2017) focused on European regional simulations, exploring the effects of a 2 °C climate change combined with anthropogenic emission changes in an ensemble of four models. Similarly, Fortems-

Cheiney et al. (2017) explored the same scenarios for a 3 °C climate change, with a focus on gaseous species, and Carvalho et al. (2010) conducted a SRES (Special Report on Emission Scenarios) A2 climate change scenario over the end of the 21st century for Europe, zooming on Portugal. The common point of all these studies is that all of the impacting factors were changed simultaneously in a future scenario. A review of existing scenarios is presented in Colette et al. (2015).

Unlike these studies, other papers have investigated the impact of emissions and meteorology on the atmospheric composition in future scenarios separately. Dawson et al. (2007) focused on determining the atmospheric sensitivity to changes in meteorological conditions in the eastern US, over a simulation period of 2 months. Megaritis et al. (2014) used a similar approach to Dawson et al. (2007), exploring the sensitivity of the atmospheric composition to changes in meteorological conditions for Europe over a 3-month-long simulation period. These two studies both conducted sensitivity tests over short (month-long) periods of time. Lemaire et al. (2016) explored climate change effects using the same data set as that used in our work, and developed a statistical method to ascertain the meteorological parameters that affect atmospheric pollutants in future scenarios. Hedegaard et al. (2013) also looked at the relative importance of emissions and meteorological drivers in a hemispheric model. Finally, Colette et al. (2013) explored the same scenarios that we worked on with the aim of analyzing the global effects of the three drivers (meteorology, emissions and boundary conditions) on atmospheric composition, although they only focused on Europe as a whole and did not investigate the individual effects of the drivers on PM composition. Our aim is to complement these previous studies by providing a deeper insight into the respective impacts of climate, atmospheric composition and emission-related forcing. This is why the work described here focuses on simulating a set of future and climatic scenarios over long periods of time, and observing the differences between the drivers discussed above. The chosen approach is to change the drivers one by one and assess the differences induced in PM components in order to investigate the individual effects of the parameters in the simulation. Finally, the simulations are compared with a series of simulations for which all of the aforementioned drivers change at the same time; this can show us the overall impact of all of the drivers, which may be different to the sum of the impacts of individual drivers due to nonlinear effects.

It should be noted that other studies have also explored the dependence of PM components on meteorological conditions (Dawson et al., 2007; Carvalho et al., 2010; Fiore et al., 2012; Jiménez-Guerrero et al., 2012; Juda-Rezler et al., 2012; Hedegaard et al., 2013; Megaritis et al., 2014). However, most of these studies were performed over short time periods, such as 1-year-long simulations (shorter in most cases), and several used sensitivity tests and not actual future scenarios to assess the changes in different meteorological parameters. Conversely, Lemaire et al. (2016) explored the sensitivity of ozone and $PM_{2.5}$ to different meteorological parameters, using 30 years of RCP8.5 scenario simulations; however, they did not consider the relationship between the speciation of PM components and these parameters in detail. To the best of our knowledge, the sensitivity of PM components to meteorological parameters for a data set this extensive containing multiple scenarios and the calculation of the effects of different drivers on same data pool has not been investigated to date.

In this paper, after a brief introduction to the simulations and the modeling framework, the impacts of different drivers are explored. The analysis first deals with climate impacts, before the effects of long-range transport and emission changes are discussed. Finally, the impact of each of these three drivers on the concentration of $PM_{10}$ and its components is calculated. The discussion of the results is divided into two parts corresponding to the geographic area: the European and the Mediterranean subdomains. Finally, a prospective view of what the PM component concentrations in the Mediterranean Basin may be like at the end of the 21st century is given.

## 2 Method

In this section, we introduce the architecture of the modeling framework, with a focus on the most sensitive component – the chemistry transport model. We also provide references to the input data used by the CHIMERE model in terms of future scenarios and for the various combinations of input parameters.

### 2.1 Modeling framework

The assessment of the long-term evolution of air quality in the context of a changing climate is performed using a suite of deterministic models following the framework introduced by Jacob and Winner (2009). Global climate projections are obtained from a global circulation model (GCM) that feeds a global chemistry transport model and a regional climate model. Finally, the latter two drive a regional chemistry transport model. The setup used in this study is presented in detail in Colette et al. (2013, 2015).

The global circulation model is the IPSL-CM5A-MR large-scale atmosphere–ocean model (Dufresne et al., 2013). It provides input to the regional climate model and the global chemistry transport model with global meteorological fields. It uses LMDZ (Hourdin et al., 2006) as its meteorological model, ORCHIDEE (Krinner et al., 2005) as its land surface model, and NEMO (Madec and Delecluse, 1998) and LIM (Fichefet and Maqueda, 1999) as the respective oceanic and sea-ice models. The horizontal resolution of this global model is $2.5° \times 1.25°$ with 39 vertical levels. For each scenario, the corresponding RCP is used for the anthropogenic

radiative forcing. The Weather Research and Forecasting model (WRF, Wang et al., 2015) is used as the regional climate model (RCM). The regional climate simulations were part of EURO-CORDEX (Jacob et al., 2014) with a spatial resolution of 0.44°. The historic simulations were evaluated by comparison with experimental data (Menut et al., 2012; Kotlarski et al., 2014; Katragkou et al., 2015). The LMDZ-INCA (Hauglustaine et al., 2014) global CTM is used for the production of chemical initial/boundary conditions for the regional CTM. The LMDZ-INCA runs used in this study have been analyzed in Szopa et al. (2013) and Markakis et al. (2014), and intercomparisons of the same runs with other global chemistry transport models have been analyzed in Shindell et al. (2013) and Young et al. (2013) in the framework of the ACCMIP (Atmospheric Chemistry and Climate Model Intercomparison) experiment. Monthly climatological fields are used as the boundary condition inputs, as the background changes over long periods of time and it was not possible to store hourly global model output to create hourly varying boundary conditions. This induces an unavoidable inconsistency between meteorology and dust fields.

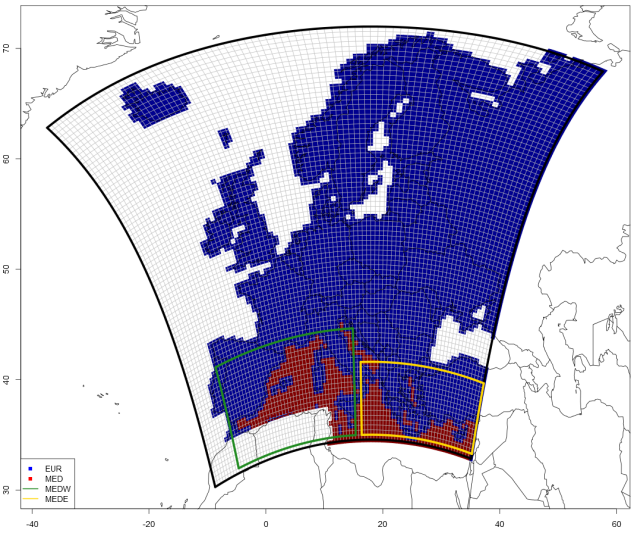


**Figure 1.** Extension of the main domain and subdomains. Four subdomains are used in this study: EUR – containing only continental Europe (blue cells), MED – containing only the Mediterranean Sea (red cells), MEDW – western Mediterranean region (green rectangle), and MEDE – eastern Mediterranean region (yellow rectangle).

## 2.2 CHIMERE CTM

The CHIMERE offline regional CTM has been widely used for both future scenarios (Colette et al., 2015; Lacressonnière et al., 2016) and for research activities in France (Zhang et al., 2013; Petetin et al., 2014; Menut et al., 2015; Rea et al., 2015; Cholakian et al., 2018) and abroad (Hodzic and Jimenez, 2011). In this work, the 2013b version of the model was used for all simulations (Menut et al., 2013). The simulations were conducted using the EURO-CORDEX domain with a horizontal resolution of 0.44° and nine vertical levels ranging from the surface to 500 mb. The aerosol module was run with a simple two-product scheme for the simulation of secondary organic aerosols (SOA, Bessagnet et al., 2008) and with the ISORROPIA module for the simulation of inorganic aerosols (Fountoukis and Nenes, 2007). It provides simulated aerosol fields including EC (elemental carbon), sulfate, nitrate, ammonium, SOA, dust, salt and PPM (primary particulate matter other than those mentioned above) considering coagulation, nucleation and condensation processes, as well as wet and dry deposition. The same unchanged land use data from GlobCover (Arino et al., 2008) with a base resolution of 300 m × 300 m have been used in different series of simulations. Dust emissions are taken into account inside the simulation domain based on the method proposed by Marticorena and Bergametti (1995).

The simulation domain has a 0.44° resolution (Fig. 1). The analysis was performed using the subdomains presented in Fig. 1. The EUR subdomain only concerns the European continent (including the British Isles), and a land–sea mask was used to remove other parts of the domain. The MED subdomain was also produced using a land–sea mask, but this time it only contained the Mediterranean Sea. The MEDW and MEDE are the last two subdomains. They refer to the western and eastern Mediterranean areas, respectively. It is important to bear in mind that these two subdomains, contrary to the previous subdomains, contain both land and sea for the purpose of observing the effects of enclosing land on the Mediterranean area. Due to this setup, the sum of MEDW and MEDE is different to that of MED.

## 2.3 Climate scenarios

Representative concentrations pathway scenarios (RCPs) designed for the fifth IPCC report (Meinshausen et al., 2011; van Vuuren et al., 2011b) are used in this study. Simulations using three of these CMIP5 RCPs (Taylor et al., 2012; Young et al., 2013) are selected: RCP2.6, RCP4.5 and RCP8.5, which consider 2.6, 4.5 and 8.5 $W m^{-2}$ of radiative forcing at the end of the 21st century, respectively. It is worth noting that RCP8.5 includes the least mitigation policies by far compared with the other two scenarios; therefore, RCP8.5 results in a high radiative forcing at the end of the century, with a temperature increase of between 2.6 and 4.8 °C for Europe according to the EEA (European Environmental Agency[1]). On the contrary, the RCP2.6 scenario considers a radiative forcing value that leads to a low-range temperature increase by 2100 (between 0.3 and 1.7 °C). This means that this scenario has to consider ambitious greenhouse gas emission reductions as well as carbon capture and storage. The RCP4.5 is an intermediate scenario with less stringent climate mitiga-

[1] https://www.eea.europa.eu/data-and-maps/indicators/global-and-european-temperature-8/assessment, last access: 21 July 2018.

tion policies, which results in a temperature increase somewhere between the two previously mentioned extreme scenarios.

### 2.4 Air pollutant emissions

The biogenic emissions input is obtained from the Model of Emissions of Gases and Aerosols from Nature (MEGAN v2.04; Guenther et al., 2006). It is worth mentioning that the emission factors and the leaf area index (LAI) values provided by this model are the same for all simulations; however, as many of the biogenic gases have a temperature-dependent nature, their emissions increase with higher temperatures. The MEGAN version used in CHIMERE takes six biogenic volatile organic compound (BVOC) emissions into account (isoprene, $\alpha$-pinene, $\beta$-pinene, humulene, limonene and ocimene) and their dependence on temperature, solar radiation and the LAI.

Anthropogenic emissions are taken from the ECLIPSE-V4a global emissions projections (Amann et al., 2013; Klimont et al., 2013, 2017). This database covers the 2005–2050 time period with two main prospective pathways: the current legislation emissions (CLE) and the maximum feasible reduction (MFR) scenarios. These two scenarios show the effects of minimum and maximum mitigation efforts that can be expected by 2050, which gives us a spectrum of possible influences of anthropogenic emissions in future scenarios. For both scenarios, the atmospheric emissions of the main anthropogenic pollutants are available as global maps at a resolution of $0.5\,^{\circ}$.

The simulations used in this study are summarized in Table 1. As the goal of this study is to separately investigate the regional CTM drivers that can affect the results of future simulations, different series of simulations were performed, with each one allowing for the evaluation of climate, anthropogenic emission and boundary condition impacts on PM concentrations.

As for the climate impact study, RCP2.6, RCP4.5 and RCP8.5 scenarios are used in combination with constant anthropogenic emissions and identical boundary conditions. These scenarios are compared with the historic simulations.

In order to explore the changes induced by boundary conditions on the CTM outputs, RCP4.5 scenarios were conducted using two different sets of boundary conditions from the same global CTM and compared with historic simulations. The difference between these two sets of conditions is the fact that anthropogenic pollutants from the RCP emissions (emissions produced for RCP scenarios exclusively) are used as anthropogenic inputs for one of them (Szopa et al., 2006, 2013), whereas the other one relies on ECLIPSE-V4a emissions as inputs (Markakis et al., 2014).

The emission impact study uses the RCP4.5 climate forcing with CLE 2010, CLE 2050 and MFR 2050 anthropogenic emissions, with each one again being compared with historic simulations.

As seen in Table 1, we simulated different prospective periods in the different series of simulations. In the case of the climate impact studies, a 30-year-long historical simulation and 70-year-long future simulation were used for each future scenario. As for the other simulations, 10 years of historical simulations (1996 to 2005) were compared with 10 years of future scenarios, representing the 2050s (2045 to 2054). This latter period was chosen because it is centered on year 2050, for which CLE/MFR 2050 emissions are available. In the end, a 10-year-long simulation was performed during which all of these factors were simultaneously changed. We have to mention that it would have been numerically too strenuous to perform 70 years of simulations for emission/boundary condition drivers, bearing in mind that the climatic impact simulations already amount to 240 years of simulations.

A validation of our historic simulations is presented in Menut et al. (2012) and Kotlarski et al. (2014) for the meteorological parameters, whereas a validation of some chemical species is presented in the Supplement to this article (Sect. S1). This validation uses an annual profile of 10 years of historic simulations from 1996 to 2005 (with 2010 constant anthropogenic emissions) compared with an annual profile of all available measurements from EEA and air base stations between 2005 and 2015 (EEA, 2016).

## 3 Climate impacts

This section discusses the comparisons between the simulations using RCP2.6, RCP4.5 and RCP8.5 with historic simulations (simulations 1 to 4 in Table 1). As all of the inputs except the meteorological fields remain identical in these four series of simulations, it is possible to disentangle the effects of climate alone on the PM concentration in different RCPs. While the specific goal of the paper is to focus on the PM changes in the Mediterranean area alone, a general overview of the European domain is also provided. Before exploring PM changes, temperature changes are analyzed as they imply important effects on biogenic volatile organic compound (BVOC) emissions; these emissions are precursors for the production of SOAs and affect gas–particle phase partitioning in simulations. The dependency of total $PM_{10}$ and its components on other meteorological parameters is also discussed in detail in this section.

### 3.1 Meteorological parameters

The RCP2.6 reaches its maximum radiative forcing ($2.6\,W\,m^{-2}$) in the 2040s (van Vuuren et al., 2011a), meaning that an increase in radiative forcing is seen in this scenario until this decade, whereas afterwards we observe a continuous decrease. Therefore, in the bulk of the RCP2.6 simulations over Europe, a temperature decrease appears from about 2050 onwards, followed by a new increase in temperature over the last 10 years simulated (Fig. 2). As for the

**Table 1.** The different scenarios used in this work.

| | No. | Simulation name | Simulation period | Global chemistry model | Regional climate model | Anthropogenic emissions |
|---|---|---|---|---|---|---|
| Climate | 1 | Hist | 1976–2005 | LMDZ-INCA-RCP2.6 ECLIPSE emissions | WRF Historic | ECLIPSE-V4a CLE2010 |
| | 2 | RCP2.6 | 2031–2100 | | WRF RCP2.6 | |
| | 3 | RCP4.5 | 2031–2100 | | WRF RCP4.5 | |
| | 4 | RCP8.5 | 2031–2100 | | WRF RCP8.5 | |
| Boundary conditions | 5 | RCP4.5-BC | 2046–2055 | LMDZ-INCA-RCP4.5 RCP emissions | WRF RCP4.5 | ECLIPSE-V4a CLE2010 |
| Emissions | 6 | RCP4.5-CLE2050 | 2046–2055 | LMDZ-INCA-RCP2.6 ECLIPSE emissions | WRF RCP4.5 | ECLIPSE-V4a CLE2050 |
| | 7 | RCP4.5-MFR2050 | 2046–2055 | | | ECLIPSE-V4a MFR2050 |
| All | 8 | RCP4.5-BC-CLE2050 | 2046–2055 | LMDZ-INCA-RCP4.5 RCP emissions | WRF RCP4.5 | ECLIPSE-V4a CLE2050 |

RCP4.5 scenario, this maximum radiative forcing is reached in the 2070s (Thomson et al., 2011), whereas such a maximum is not reached for RCP8.5 until the end of the century. As a consequence, the temperature increase levels out after about 2070 in RCP4.5, while the temperature keeps increasing over the whole period in RCP8.5. These elements explain the larger similarities between RCP4.5 and RCP8.5 as well as their structural differences with RCP2.6. The time evolutions are similar for the European (EUR) and Mediterranean (MED) domains, albeit absolute temperatures are nearly 10 °C warmer over the Mediterranean on average (Fig. S2 for 2-D temperature fields).

In the following comparisons, annual average values over each subdomain and for each parameter and time series corresponding to 30 years of historic simulations and 70 years of future scenarios are presented. The uncertainties associated with each value account for the spatial variability of each parameter.

The 2 m temperatures are generally higher for the Mediterranean area than for the European continent; however, the increase in temperature is more pronounced for EUR than for MED (+1.69, +2.63 and +3.62 °C for EUR and +1.06, +1.72 and +2.91 °C for MED for RCP2.6, RCP4.5 and RCP8.5, respectively). In the other two Mediterranean subdomains temperature changes are higher for MEDE than for MEDW (+1.25, +2.05 and +3.38 °C for MEDE and +0.73, +1.77 and +2.88 °C for MEDW for RCP2.6, RCP4.5 and RCP8.5, respectively). While the European subdomain shows a more important temperature increase in winter (+1.86, +3.44 and +4.42 °C for RCP2.6, RCP4.5 and RCP8.5, respectively), the Mediterranean subdomains show a larger increase in summer (for MED +1.40, +2.06 and +3.22 °C for RCP2.6, RCP4.5 and RCP8.5, respectively). Maps of differences in temperature for the different scenarios and seasons are presented in the Supplement (Fig. S2). It should be noted that the average temperature changes discussed here agree with the literature (Knutti and Sedláček, 2012; Vautard et al., 2014).

As seen in Fig. 2, some of the parameters behave differently in the two subdomains. For example, for the amount of precipitation, an increase is simulated in EUR for RCP8.5, whereas a slight decrease is simulated for RCP2.6 after the 2050s, which makes precipitation stronger in RCP8.5 than in RCP2.6 on average for the future period. In the MED area, the opposite behavior is generally noted: precipitation is stronger in RCP2.6 than in RCP8.5. On the contrary, there is a steady decrease in the total duration of rain hours (sum of hours rained each year in each scenario – a threshold that is fixed for each subdomain using the average of 25th percentile for the whole duration of simulations). Therefore, rain events are expected to become more intense (Vautard et al., 2014). Regarding the total duration of rain hours in the Mediterranean region, the same result is obtained as for the EUR region, except for the RCP2.6 scenario where an increase in the number of rainy hours is simulated. This increase corresponds to the western basin of the Mediterranean Sea. For the eastern basin, all scenarios show a decrease in this parameter (Fig. S3 for MEDW and MEDE).

The same type of comparison is performed for wind speed (WS; 10 m wind), relative humidity (RH) and planetary

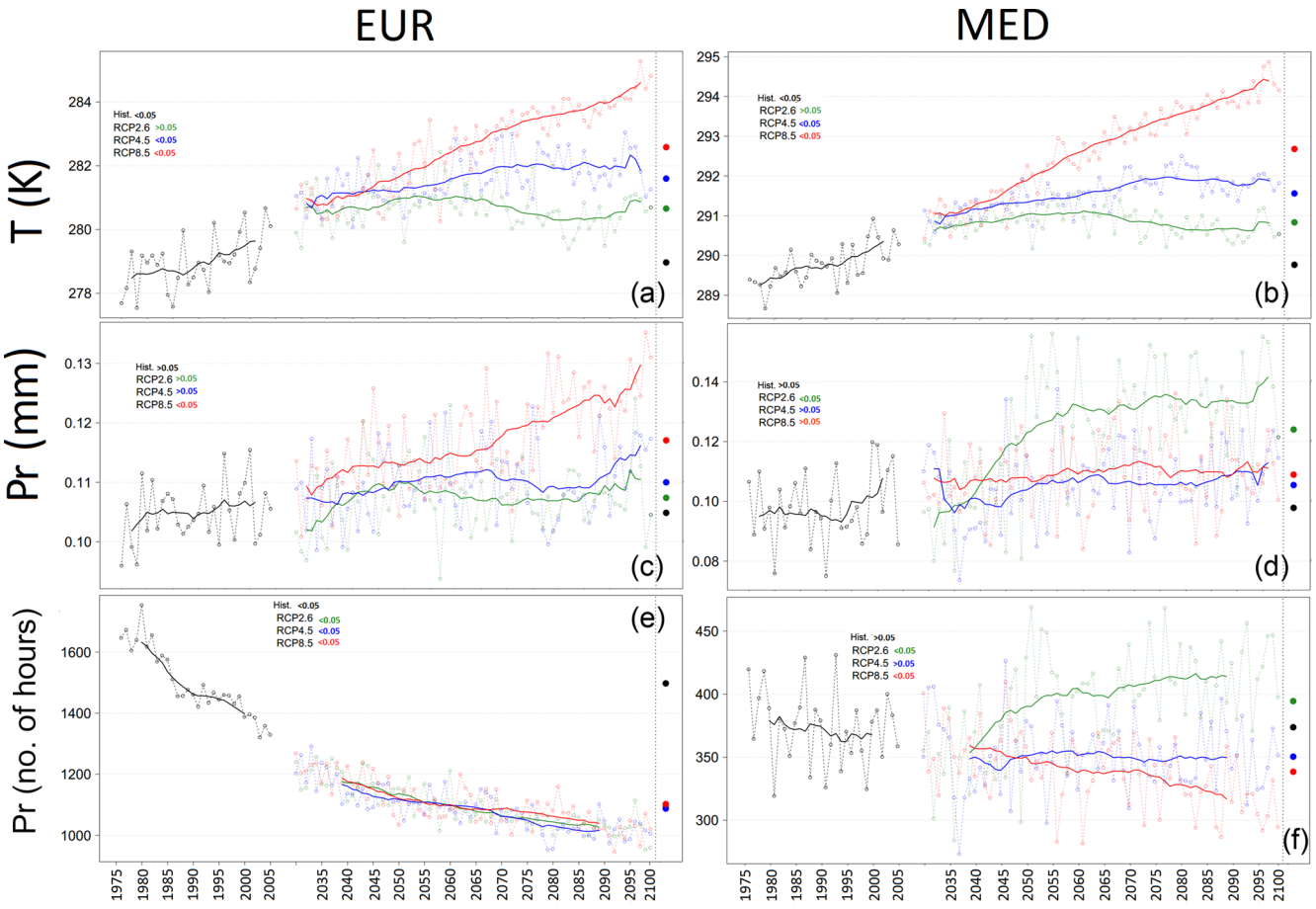


**Figure 2.** Time series of temperature (K; **a**, **b**), precipitation (mm; **c**, **d**) and number of rainy hours (**e**, **f**) for EUR (**a**, **c**, **e**) and MED (**b**, **d**, **f**) subdomains for all climate change scenarios as well as historic simulations. The average for each scenario is shown by the corresponding point on right side of the plot. The solid lines show the rolling average of 30 years for future scenarios and 20 years for historic scenarios. Numbers in the legend show the $p$ value of the linear regression for each scenario.

boundary layer height (PBLH) in Fig. 3 for the EUR and MED areas. RH remains rather constant without a significant trend over EUR and MED, with the exception of the RCP2.6 scenario for MED which shows a significant decrease. WS mostly shows nonsignificant trends, with the exception of the RCP2.6 scenario over the MED domain. Similar results for WS changes have also been seen in other studies (Dobrynin et al., 2012; de Winter et al., 2013). Finally, PBLH increases are significant for RCP8.5 over EUR and for RCP2.6 over MED.

These meteorological parameters undergo interactions between themselves and show correlations with each other, as they are driven by circulation patterns. The values of correlations between different meteorological parameters examined in this work are shown in Supplement (Sect. S4). The main points that should be taken into account regarding cross-correlations between meteorological parameters are the positive correlations between wind speed and the PBLH, between wind speed and precipitation and also the anti-correlation between wind speed and RH. All of these correlations are above 0.6 as an absolute value.

Also it should be noted that if the GCM used to provide the boundary conditions to the regional climate model was changed, the results seen here might be different (Olesen et al., 2007; Teichmann et al., 2013; Kerkhoff et al., 2015; Lacressonnière et al., 2016).

### 3.2 $PM_{10}$ concentrations

The simulated $PM_{10}$ concentrations are shown in Fig. 4 for the EUR and MED subdomains. The differences between future (2031–2100) and historical (1976–2005) simulations are presented, with historical simulations being used as a reference. Compared with historical simulations, we observe a decrease in $PM_{10}$ for all scenarios, for both EUR ($0\pm0.95$ %, $-2.57\pm0.90$ % and $-4.40\pm0.87$ % for RCP2.6, RCP4.5 and RCP8.5, respectively) and MED ($0.9\pm0.09$ %, $-5.65\pm0.11$ % and $-8.10\pm0.12$ % for RCP2.6, RCP4.5 and RCP8.5, respectively). The uncertainties shown here and in

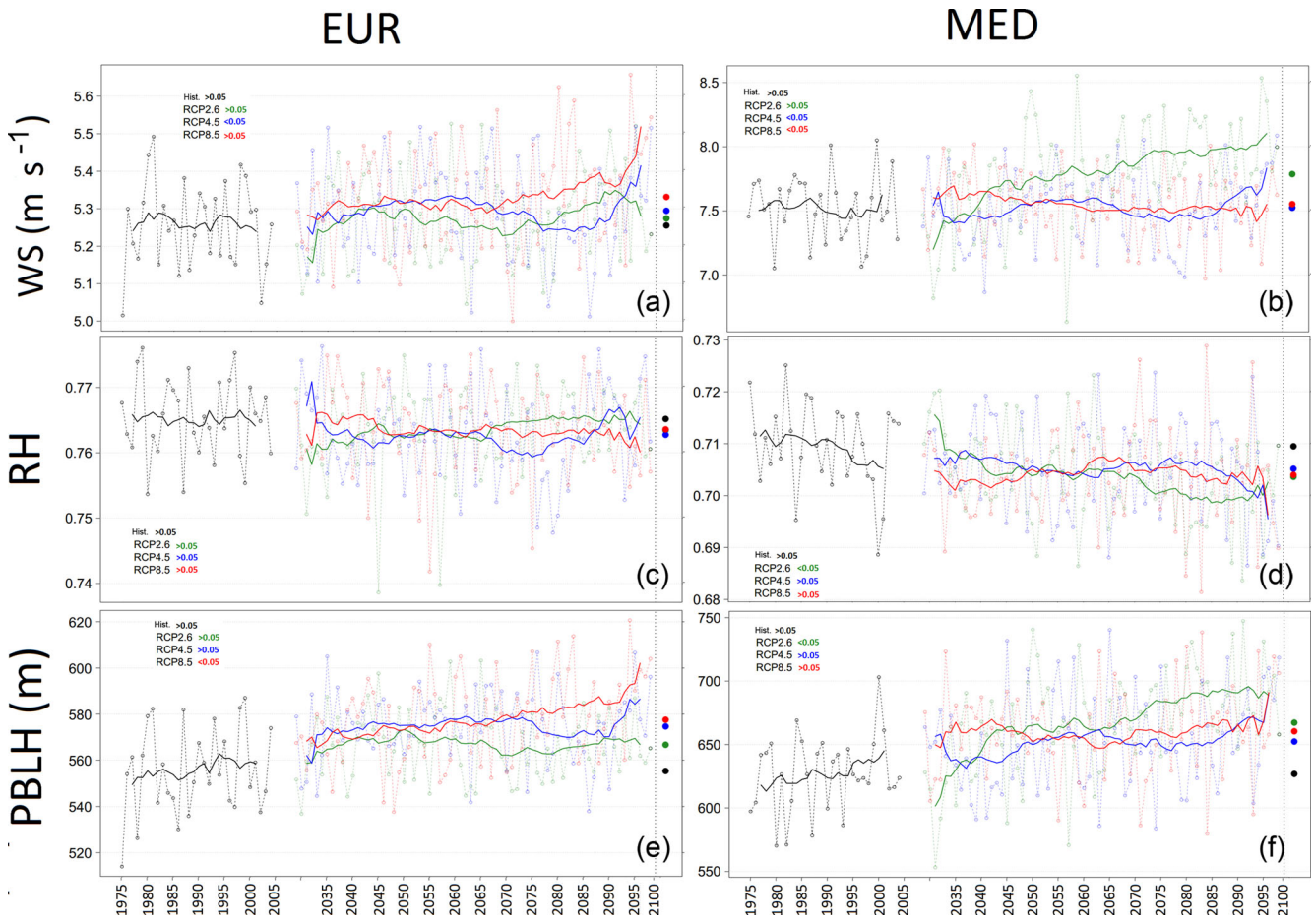


**Figure 3.** Time series of wind speed (WS; $m\,s^{-1}$; **a, b**), relative humidity (RH; **c, d**) and planetary boundary layer height (PBLH; in meters; **e, f**) for EUR **(a, c, d)** and MED **(b, d, f)** subdomains for all climate change scenarios as well as historic simulations. The average for each scenario is shown by the corresponding point on right side of the plot. The solid lines show the rolling average of 30 years for future scenarios and 20 years for historic scenarios. Numbers in the legend show the $p$ value of the linear regression for each scenario.

the rest of the document refer to spatial 1-sigma intervals. The reasons for these changes in $PM_{10}$ are discussed in the next subsection by analyzing individual PM components.

Alternatively, we also calculate linear trends for the future periods. A statistically significant positive trend is observed for RCP2.6 in the future, whereas it is significantly negative for RCP8.5, and nonsignificant for RCP4.5 ($p$ values are given in Fig. 4 for linear trend lines).

Evidently, $PM_{10}$ has a seasonal variation which is shown in Fig. 5; box plots of $PM_{10}$ for all four seasons and all four subdomains are shown in Fig. 6 (Fig. S5 for $PM_{2.5}$). Interestingly, for EUR, the general $PM_{10}$ decrease noted above for the Hist, RCP2.6, RCP4.5 and RCP8.5 scenarios is reversed in the summer period. We see that elevated concentrations of $PM_{10}$ are simulated over the Mediterranean area for all seasons, reaching their maximum in spring (Fig. 6). Another interesting result in Fig. 5 is the increasing concentrations of $PM_{10}$ over eastern Europe in summer, and over the Scandinavian and eastern European regions both in summer and winter, in RCP4.5 and RCP8.5. This increase for the summer period is due to BVOC emission increases, which are discussed in Sect. 3.4.2. However, the same effect is not seen in RCP2.6 in either of these seasons, highlighting a structural difference between RCP2.6 and the other two scenarios. These results are discussed in the light of $PM_{10}$ components and meteorological parameter covariance in Sect. 3.4. A more general explanation for these structural differences can be found in the nature of the three scenarios, caused by the previously mentioned discriminated changes in meteorological parameters (Sect. 3.1).

### 3.3 Distribution of chemical $PM_{10}$ components

Figure 7 shows the $PM_{10}$ concentrations and concentration changes for all of different scenarios and subdomains, as well as the contributions of all of the different $PM_{10}$ components (Fig. S6 for $PM_{2.5}$). For each PM component, the relative differences between future scenarios and historical simulations are also reported. Major differences can be seen

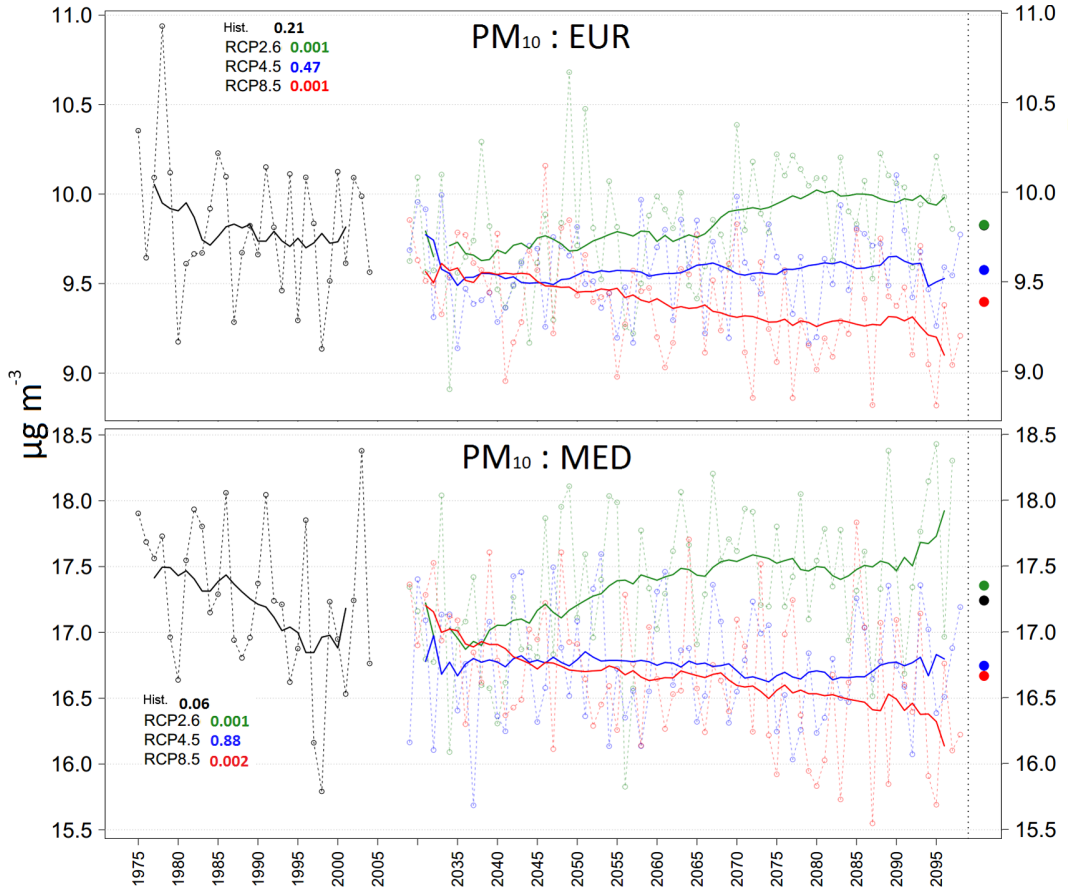


**Figure 4.** $PM_{10}$ time series for the EUR and MED subdomains for all climate change scenarios and historic simulations. The average for each scenario is shown by the corresponding point on right side of the plot. The solid lines show the rolling average of 30 years for future scenarios and 20 years for historic scenarios. Numbers in the legend indicate the $p$ value of the linear regression for each scenario.

in the distribution of the different PM components: for $PM_{10}$ the major contributors are salt and dust particles in our domains of interest, whereas their contribution to $PM_{2.5}$ is lower. Consequently, secondary inorganics ($SO_4^{2-}$, $NO_3^-$ and $NH_4^+$) and carbonaceous aerosol (black carbon, primary organic aerosol, biogenic secondary organic aerosol) are the major contributors to $PM_{2.5}$ (Fig. S6).

Another interesting point from this study is that primary aerosol species such as primary organic aerosols (POA), anthropogenic secondary organic aerosols (ASOA), PPM and black carbon (BC) only change slightly under a future climate (when emissions are kept constant), over both Europe and the Mediterranean Basin (a maximum of $\pm 5\,\%$ change for most of them). It should be noted here that this article deals with annual averages and not extreme events; regional climate changes can have strong effects on primary pollutant peaks as is shown in Vautard et al. (2018). The evolution of these species is again discussed in Sect. 4.2 with respect to anthropogenic emission changes.

The most important changes in the future scenario outputs (with respect to historic simulations) are found to be a decrease in nitrates (for EUR $-11.2 \pm 0.8\,\%$, $-21.4 \pm 0.7\,\%$ and $-28.8 \pm 0.8\,\%$ for RCP2.6, RCP4.5 and RCP8.5, respectively) and an increase in the organic aerosol concentration (for EUR $+15.1 \pm 1.2\,\%$, $+22.7 \pm 1.3\,\%$ and $+34.9 \pm 1.3\,\%$ for RCP2.6, RCP4.5 and RCP8.5, respectively). A slight increase in sea-salt particles (for EUR $+0.8 \pm 0.05\,\%$, $+1.4 \pm 0.06\,\%$ and $+0.2 \pm 0.06\,\%$ for RCP2.6, RCP4.5 and RCP8.5, respectively) and in sulfates (for EUR $+4.50 \pm 0.62\,\%$, $+3.0 \pm 0.6\,\%$ and $+1.6 \pm 0.6\,\%$ for RCP2.6, RCP4.5 and RCP8.5, respectively) is also found. An interesting result regarding sulfates is that the concentration of this species displays an increase in all scenarios compared with historical simulations, although the scenario order for this increase is the inverse of that for the temperature increase (i.e., RCP2.6 > RCP4.5 > RCP8.5). This phenomena is discussed later in this section. While a decrease in dust particles is observed for RCP4.5 and RCP8.5 (for EUR $-5.6 \pm 2.4\,\%$ and $-5.3 \pm 2.2\,\%$, respectively), these particles remain almost constant in RCP2.6. A decrease is seen for the ammonium particles in all scenarios (for EUR $-2.1 \pm 0.2\,\%$, $-6.4 \pm 0.2\,\%$ and $-10.6 \pm 0.2\,\%$ for RCP2.6, RCP4.5 and

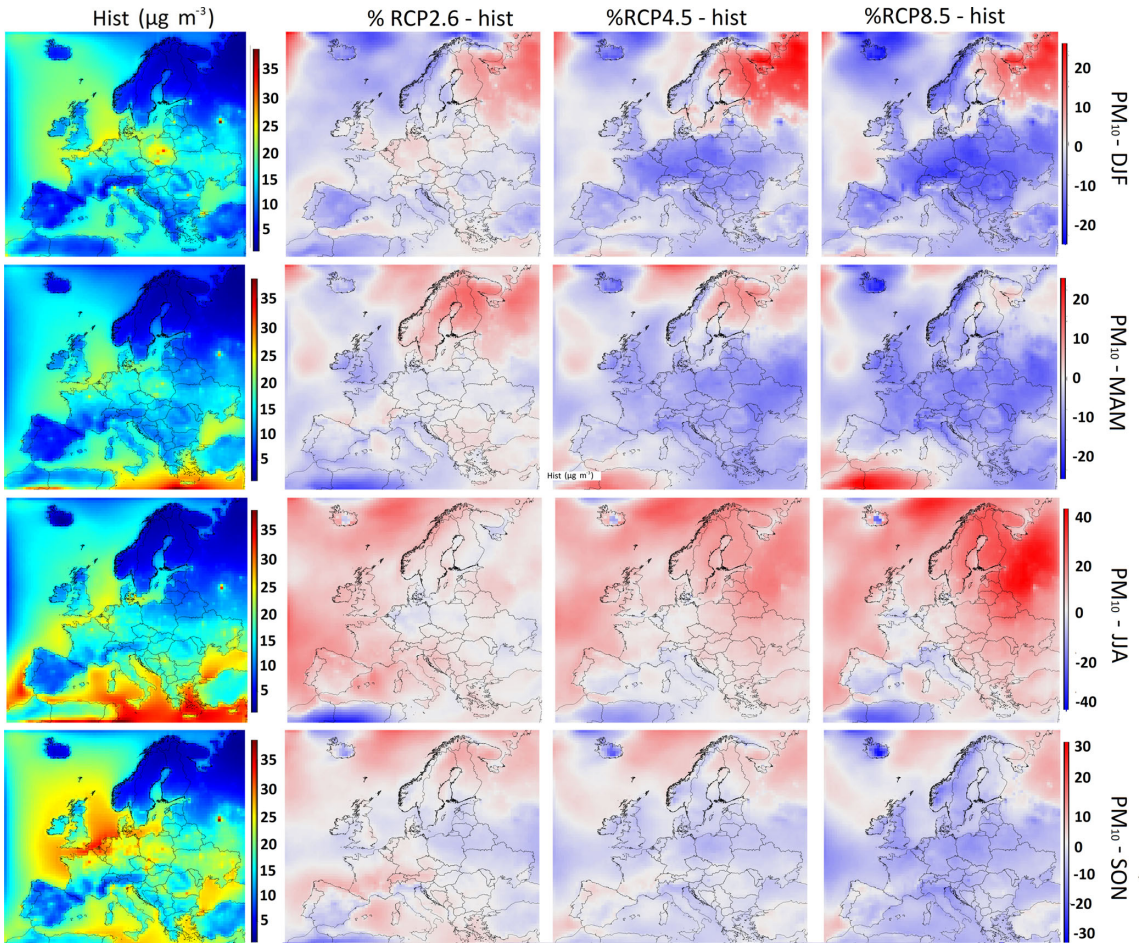


**Figure 5.** $PM_{10}$ seasonal average concentrations in the historical simulation (first column). Relative differences between the climate simulations (RCP2.6, RCP4.5 and RCP8.5) and the historical simulation (Hist) (second, third and fourth columns, respectively). Rows represents the different seasons (winter, spring, summer and fall, from top to the bottom). Please note that the scale used differs between seasons for the sake of readability.

RCP8.5, respectively). However, the main driving force for the decrease in the concentration of total $PM_{10}$ (seen in Fig. 4) for the RCP4.5 and RCP8.5 scenarios is the decrease of nitrates. The increase in the concentration of other species, especially BSOA, is compensated for by the decrease in nitrate concentrations in the case of the two abovementioned scenarios with a seasonal dependence. As for RCP2.6, as the decrease in nitrates is generally lowest among all future scenarios, the slight increase in BSOA, sulfates, dust and salt particles drives the increase in the $PM_{10}$ concentrations (Fig. 7).

In the Mediterranean area, however, the predictions appears to be quite different: in general, the aerosol burden over the Mediterranean area (MED) is higher than that over the European area (average of 9.8, 9.5 and 9.4 $\mu g\,m^{-3}$ for EUR compared with 17.4, 16.7 and 16.6 $\mu g\,m^{-3}$ for MED for RCP2.6, RCP4.5 and RCP8.5, respectively, Fig. 7). This is mainly due to sea salt (approximately 9 $\mu g\,m^{-3}$ in all scenarios) and dust (nearly 4 $\mu g\,m^{-3}$ in all scenarios). Note that the MED region, by definition, only contains grid cells over sea, which explains the large sea-salt contribution. Conversely, for this area, the concentrations of aerosols that depend on continental emissions are considerably lower (−25 %, −33 % and −32 % for BC, POAs and ammonium, respectively, in MED compared with EUR for the RCP4.5 scenario for $PM_{10}$). Nitrates also show a significantly lower concentration in this region (from 1.03 $\mu g\,m^{-3}$ for EUR to 0.21 $\mu g\,m^{-3}$, 0.39 $\mu g\,m^{-3}$ and 0.25 $\mu g\,m^{-3}$ for RCP4.5 in $PM_{10}$ for MED, MEDW and MEDE, respectively). Sulfur emissions from maritime shipping lead to high sulfate concentrations over the Mediterranean area, especially over the eastern Mediterranean (2.5 $\mu g\,m^{-3}$ in MEDE compared with 1.99 $\mu g\,m^{-3}$ in EUR for the RCP4.5 scenario for $PM_{10}$). Finally, it is worth noting that the BSOA fraction is lower over the Mediterranean (−36 %, −31 % and −23 % of BSOA compared with EUR in MED, MEDW and MEDE, respectively). The relative changes in the Mediterranean domain compared with historic simulations are close to those for the

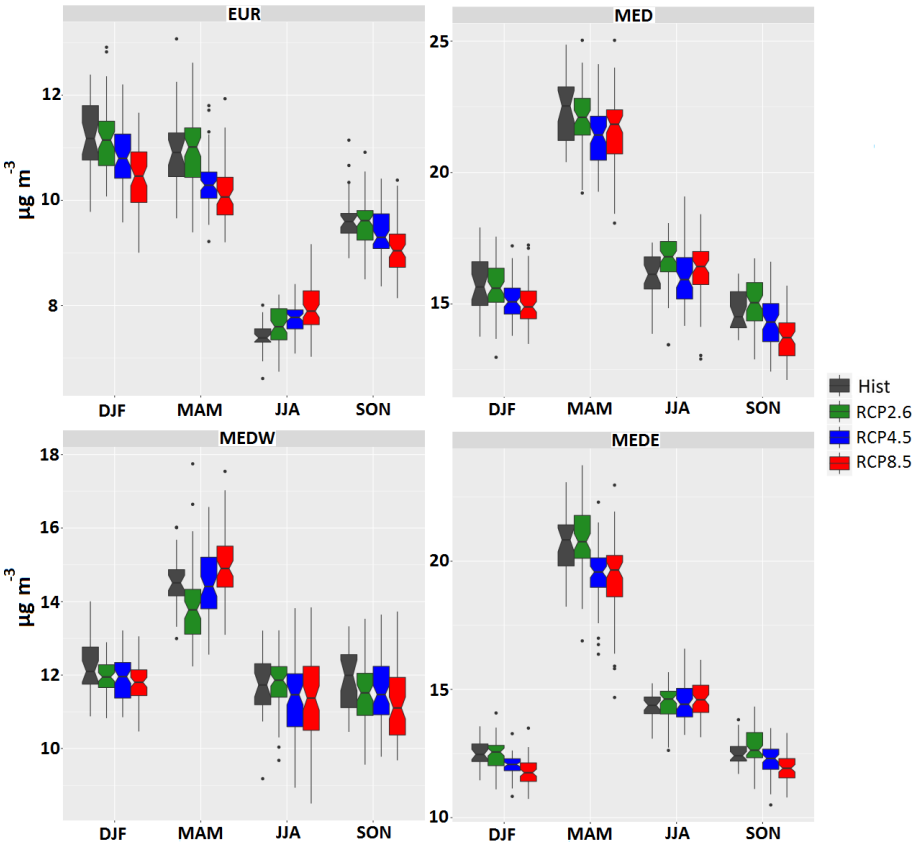


**Figure 6.** Seasonal box plots for all scenarios for all seasons for $PM_{10}$ (historic simulations are black, RCP2.6 is green, RCP4.5 is blue and RCP8.5 is red) for the different subdomains. Scales are different for different subdomains.

European subdomain for most species, although they show different intensities for most components. An interesting behavior is seen for BSOA, where the increase in the concentration of this component becomes more homogenous between the three future climatic scenarios in the Mediterranean Basin with respect to continental Europe. The reason for this behavior is the origin of BSOA from advection over the Mediterranean subdomain. Also, sulfates, while showing the same general behavior as in the European subdomain, show lower changes between future and historic simulations over the Mediterranean Basin, resulting in a decrease in concentration in the RCP8.5 scenario.

### 3.4 Dependence of $PM_{10}$ components on meteorological parameters

In order to explain the evolution of PM components under future climate scenarios, they are correlated here with different meteorological parameters. The parameters tested here are temperature, wind speed, precipitation, RH, PBLH and shortwave radiation. Because of the variations in the seasonality of the different PM components, the analysis of their dependencies on meteorological parameters must be conducted for each season separately. Figure 8 shows the seasonal changes for nitrates, sulfates, BSOA and dust particles for all subdomains. The 2-D concentration fields for nitrates, BSOA, sulfates and dust particles are shown in Fig. 9 for the season when each component shows its highest concentration (Fig. 8). The correlations for all seasons and for the five selected meteorological parameters with $PM_{10}$ components are shown in Figs. 10 and 11 for the EUR and MED subdomains for different years. This comprises 30 pairs of values for the historic period and 70 for the future period. Here, a Pearson correlation coefficient of greater than 0.6 is considered to represent a significant relationship. Correlations between the different meteorological parameters are shown in Figs. S7 and S8. Figure S9 shows the 2-D correlations for the same species as Fig. 8, with the parameter that correlates best with them for selected seasons when their concentration is highest (i.e., nitrates, BSOA, sulfates and dust with temperature, temperature, RH and PBLH for winter, summer, summer and spring, respectively).

#### 3.4.1 Inorganic PM components

Particulate nitrate concentrations appear to be strongly anticorrelated with temperature (Fig. 10). Hence, in most regions, they show a decrease in the future scenarios, mainly

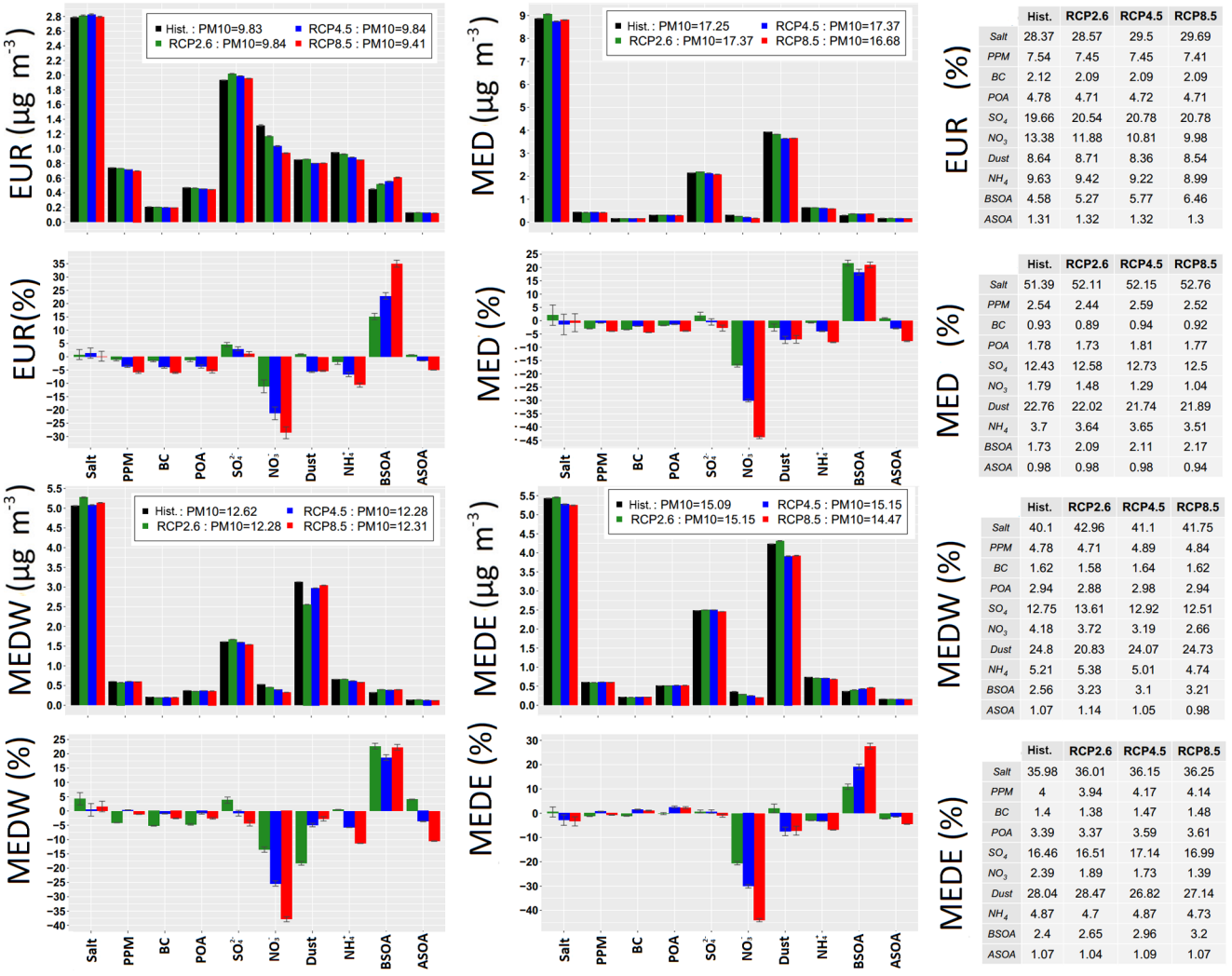


| EUR (%) | Hist. | RCP2.6 | RCP4.5 | RCP8.5 |
|---|---|---|---|---|
| Salt | 28.37 | 28.57 | 29.5 | 29.69 |
| PPM | 7.54 | 7.45 | 7.45 | 7.41 |
| BC | 2.12 | 2.09 | 2.09 | 2.09 |
| POA | 4.78 | 4.71 | 4.72 | 4.71 |
| $SO_4$ | 19.66 | 20.54 | 20.78 | 20.78 |
| $NO_3$ | 13.38 | 11.88 | 10.81 | 9.98 |
| Dust | 8.64 | 8.71 | 8.36 | 8.54 |
| $NH_4$ | 9.63 | 9.42 | 9.22 | 8.99 |
| BSOA | 4.58 | 5.27 | 5.77 | 6.46 |
| ASOA | 1.31 | 1.32 | 1.32 | 1.3 |

| MED (%) | Hist. | RCP2.6 | RCP4.5 | RCP8.5 |
|---|---|---|---|---|
| Salt | 51.39 | 52.11 | 52.15 | 52.76 |
| PPM | 2.54 | 2.44 | 2.59 | 2.52 |
| BC | 0.93 | 0.89 | 0.94 | 0.92 |
| POA | 1.78 | 1.73 | 1.81 | 1.77 |
| $SO_4$ | 12.43 | 12.58 | 12.73 | 12.5 |
| $NO_3$ | 1.79 | 1.48 | 1.29 | 1.04 |
| Dust | 22.76 | 22.02 | 21.74 | 21.89 |
| $NH_4$ | 3.7 | 3.64 | 3.65 | 3.51 |
| BSOA | 1.73 | 2.09 | 2.11 | 2.17 |
| ASOA | 0.98 | 0.98 | 0.98 | 0.94 |

| MEDW (%) | Hist. | RCP2.6 | RCP4.5 | RCP8.5 |
|---|---|---|---|---|
| Salt | 40.1 | 42.96 | 41.1 | 41.75 |
| PPM | 4.78 | 4.71 | 4.89 | 4.84 |
| BC | 1.62 | 1.58 | 1.64 | 1.62 |
| POA | 2.94 | 2.88 | 2.98 | 2.94 |
| $SO_4$ | 12.75 | 13.61 | 12.92 | 12.51 |
| $NO_3$ | 4.18 | 3.72 | 3.19 | 2.66 |
| Dust | 24.8 | 20.83 | 24.07 | 24.73 |
| $NH_4$ | 5.21 | 5.38 | 5.01 | 4.74 |
| BSOA | 2.56 | 3.23 | 3.1 | 3.21 |
| ASOA | 1.07 | 1.14 | 1.05 | 0.98 |

| MEDE (%) | Hist. | RCP2.6 | RCP4.5 | RCP8.5 |
|---|---|---|---|---|
| Salt | 35.98 | 36.01 | 36.15 | 36.25 |
| PPM | 4 | 3.94 | 4.17 | 4.14 |
| BC | 1.4 | 1.38 | 1.47 | 1.48 |
| POA | 3.39 | 3.37 | 3.59 | 3.61 |
| $SO_4$ | 16.46 | 16.51 | 17.14 | 16.99 |
| $NO_3$ | 2.39 | 1.89 | 1.73 | 1.39 |
| Dust | 28.04 | 28.47 | 26.82 | 27.14 |
| $NH_4$ | 4.87 | 4.7 | 4.87 | 4.73 |
| BSOA | 2.4 | 2.65 | 2.96 | 3.2 |
| ASOA | 1.07 | 1.04 | 1.09 | 1.07 |

**Figure 7.** Concentrations and relative changes of $PM_{10}$ components (same color code as in Fig. 6) for all subdomains averaged over the whole period of simulations in climate change scenarios and for the different subdomains. Error bars show the confidence interval calculated for the annual averages for each subdomain. The changes show (future − historic)/historic · 100. Tables report the percentage of each component in each scenario. The concentration of $PM_{10}$ in total is noted in the legend above each figure.

due to the higher temperature predicted in those scenarios, which might lead to a shift in the nitrate gas–aerosol partitioning towards the gaseous phase and more volatilization of already formed nitrate aerosols. Especially during the winter season, anti-correlations are seen with wind speed, precipitation, and PBLH, whereas a correlation is found with surface radiation. This fits with a switch from anticyclonic conditions – characterized by cold continental weather, clear skies and high solar radiation, large vertical stability and a low PBLH – to marine conditions. Continental conditions during this season indeed favor enhanced nitrate concentrations, whereas marine conditions are related to lower concentrations.

The correlation coefficient between nitrates and temperature is the lowest in summer. If we remain in our synoptic-scale framework, hot summer days favor pollution build up and accumulation, but decrease the partitioning in favor of the particle phase, so these effects compensate for each other. In spring, RH shows a high correlation with nitrate alongside temperature as higher RH favors nitrate partitioning into the particulate phase, in particular if it exceeds the deliquescence point of ammonium nitrate (RH > 50 %). These hypotheses are supported by the correlations presented in Sect. S4, which show the correlations between the different meteorological parameters. For the MED region, a strong anti-correlation is still observed, especially for winter and spring. However, the (anti)correlations with other meteorological parameters are less pronounced and not necessarily in the same direction as for EUR, as the distinction between continental and maritime conditions is not valid for this region. Overall, the analysis suggests that the major point to be taken into account

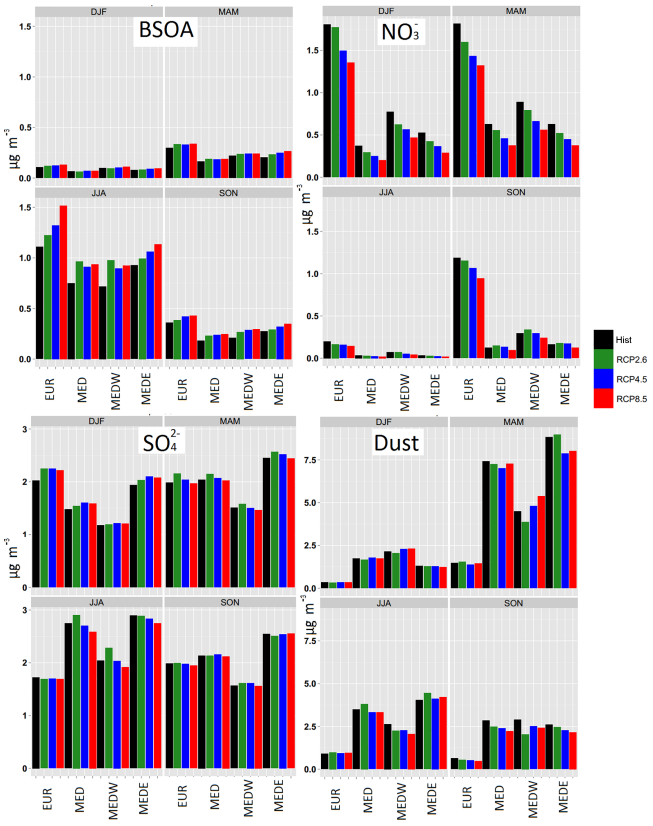


**Figure 8.** Seasonal absolute concentrations of BSOA, nitrate ($NO_3$), sulfate ($SO_4^{-2}$) and dust particles (same color code as in Fig. 5) for the different subdomains. Each panel shows one of the species mentioned above for four scenarios and each subpanel shows one season.

for particle nitrates is their high anti-correlation with temperature (seen in Fig. 10). This confirms the results reported by Dawson et al. (2007), Jiménez-Guerrero et al. (2012) and Megaritis et al. (2014), who conducted sensitivity studies on individual meteorological parameters.

Sulfates are the second most abundant species in Europe after sea salt, and the third most important species after sea salt and dust over the Mediterranean. They show an increase in all of the future scenarios compared with historical simulations, but in the inverse order of the degree of severity projected for temperature increase, i.e., the increase is strongest for RCP2.6 (5 %) and less pronounced for RCP8.5 (1.2 %) as seen in Fig. 7. The spatial distribution of this species varies quite strongly between the RCP2.6 scenario and the RCP4.5 and RCP8.5 scenarios (Fig. 9). For instance, in RCP2.6, sulfate increases with respect to historic in the southwest part of the domain, whereas it decreases for the same area in RCP4.5 and RCP8.5. The 2-D correlation maps of sulfates with RH show a strong correlation between these two parameters, especially for the Mediterranean and the Atlantic, but also for the EUR subdomain in winter and spring periods (Fig. S9). The positive relationship between sulfates and RH could be related to two different processes. First, during the winter season, the major pathway of $SO_4^{2-}$ formation from $SO_2$ proceeds via aqueous chemistry, and large-scale RH values are a tracer of sub-grid-scale cloud formation (Seinfeld and Pandis, 2016). On the contrary, during summer, over the MED region, gas-phase $SO_4^{2-}$ formation via $SO_2$ oxidation by OH is dominant, and increased future RH levels, along with increasing temperatures, may lead to increased OH levels (Hedegaard et al., 2008). However for summer and fall, the PBLH shows a higher correlation with sulfate, which is shown in Fig. 10. Another parameter that shows a strong anti-correlation with sulfate concentrations is the wind speed in the spring and winter periods, which can be explained by the correlation between the PBLH and wind speed (Fig. 10).

Ammonium concentrations show a steady decrease in all future scenarios and in all subdomains. The correlations of $NH_4^+$ with meteorological variables appear to be a combination of those simulated for $SO_4^{2-}$ and $NO_3^-$ with which $NH_4^+$ forms inorganic aerosol. When looking at correlations, a relationship is seen for ammonium with RH and wind speed, as well as a strong correlation with the PBLH (Fig. 11).

### 3.4.2 Biogenic SOA

BSOA concentrations show a steady increase in future scenarios for the European subdomain (Figs. 8 and 9). While the increase is seen in all subdomains, the intensity and the scenario dependence are not the same. The formation of the biogenic organic aerosol fraction greatly depends on its precursors (isoprene and monoterpenes), for which emissions increase globally with temperature. In EUR, isoprene emissions increase by 20.3 %, 31.1 % and 52.5 %, and monoterpenes emissions increase by 15.7 %, 24.0 % and 38.1 % for RCP2.6, RCP4.5 and RCP8.5 , respectively. There are many studies that have investigated the changes in BVOC emissions in the future; however, not many of them have only taken the climate effects into account. For example, Lathière et al. (2005) used the full version of MEGAN (which includes $CO_2$ inhibition and the dependence of isoprene emissions on ozone concentrations) to calculate a 27 % and 51 % increase in isoprene and monoterpenes, respectively, in 2100 compared with the 1990s using a scenario that is close to RCP4.5. Compared with our study, these values are quite similar for isoprene but more than double what we found for monoterpenes. Pacifico et al. (2012) calculated a 69 % increase in isoprene using a RCP8.5 scenario in 2100 compared with the 2000s, Hantson et al. (2017) found a 41 % / 25 % ratio in 2100 compared with 2000 for isoprene/monoterpenes, respectively, using RCP4.5. Langner et al. (2012) explored four different models for the European region (DEHM, EMEP, SILAM and MATCH) finding a 21 %–26 % isoprene increase; the increase in isoprene emissions in our simulations for the same period amounts to 21 %. Therefore, our simulations are consistent with the abovementioned results. In general, isoprene and monoterpene emis-

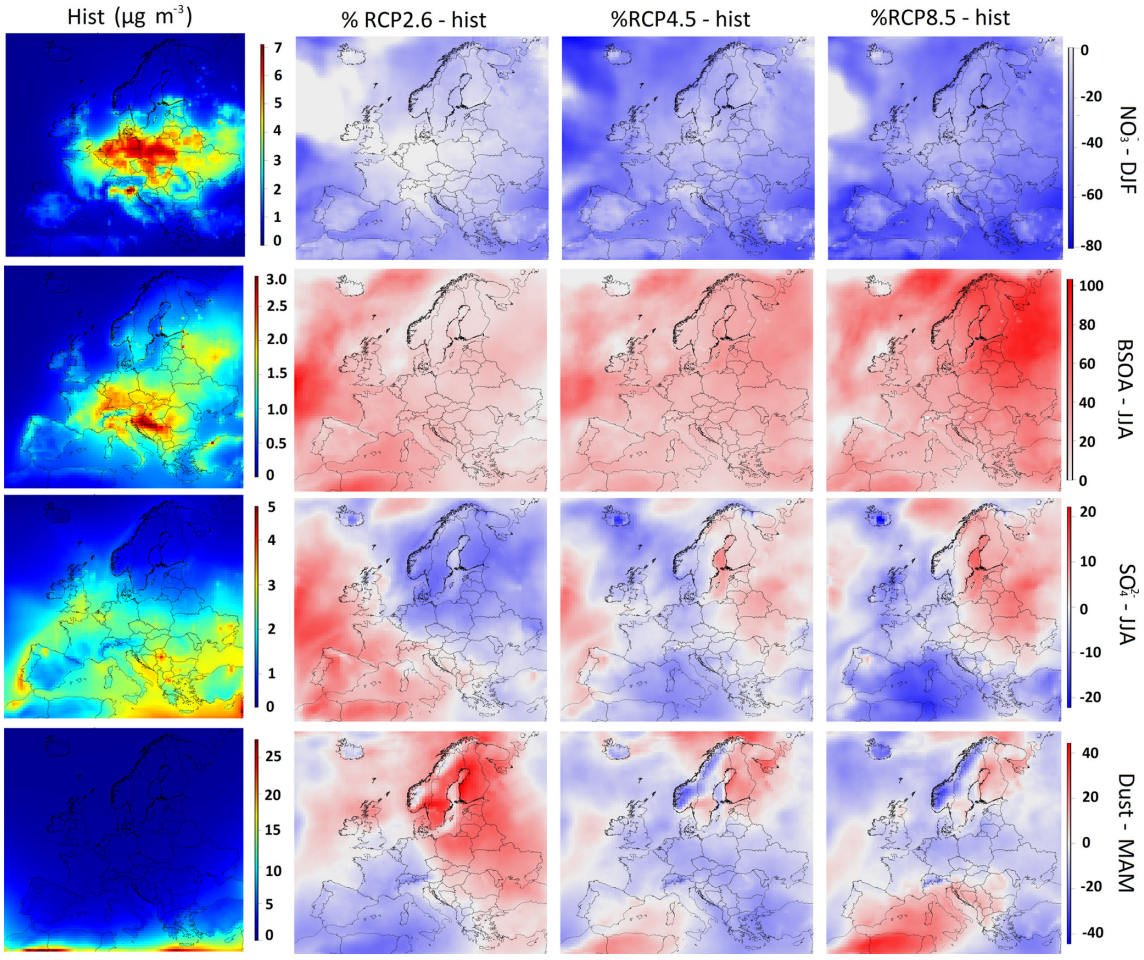


**Figure 9.** Historic concentrations and relative changes in future scenarios for biogenic SOA (BSOA), nitrates ($NO_3^-$), sulfate ($SO_4^{2-}$) and dust particles for selected seasons in which the concentrations were the highest. Figures in the left column show the average concentration of historic simulations, the other three columns show the relative difference of RCP2.6, RCP4.5 and RCP8.5 future scenarios, respectively, to the historic simulations. Each row shows one season, and the scales are different for each row of simulations.

sions show high sensitivity to temperature, $CO_2$ inhibition (Arneth et al., 2007; Young et al., 2009; Tai et al., 2013) and land use changes, which makes their estimation for future scenarios highly uncertain.

This increase in precursors results in an increase in the concentration of BSOA (for EUR 15.1 %, 22.7 % and 34.9 % for RCP2.6, RCP4.5 and RCP8.5, respectively), with a similar effect having been predicted in other studies (Heald et al., 2008; Megaritis et al., 2014). This increase in BSOA also reflects the summer increase in the $PM_{10}$ mentioned in Sect. 3.2. However, higher temperatures induce higher evaporation for semivolatile organic compounds, and, therefore, lower formation of organic aerosols is to be expected. This fact has been shown in Dawson et al. (2007), where without changing biogenic emissions, the temperature was increased by 5 °C and a decrease of almost 20 % was seen for the SOA concentration over the eastern US. In our simulations, the increase in biogenic precursors resulting due to the formation of BSOA trumps the evaporation effect due to higher temperature, and an increase in biogenic SOA is seen. Figure 10 shows the correlation coefficient of BSOA with temperature for the EUR and MED subdomains (see Fig. S9 for spatial correlations). For the EUR subdomain, statistically significant regressions are seen for all scenarios during summer for temperature and also for shortwave radiation. For the Mediterranean subdomains, no monoterpenes or isoprene are emitted from the sea surface; therefore, the concentration of BSOA in the Mediterranean area is the result of transport from the continental area. This results in low correlations between temperature and BSOA for the Mediterranean subdomains, whereas a high correlation is found between wind speed, RH and PBLH. The correlation of the BSOA concentration with wind speed in the Mediterranean corresponds to the point raised above regarding the advective nature of BSOA concentrations in this subdomain, whereas the high correlations of PBLH and RH with BSOA come from the

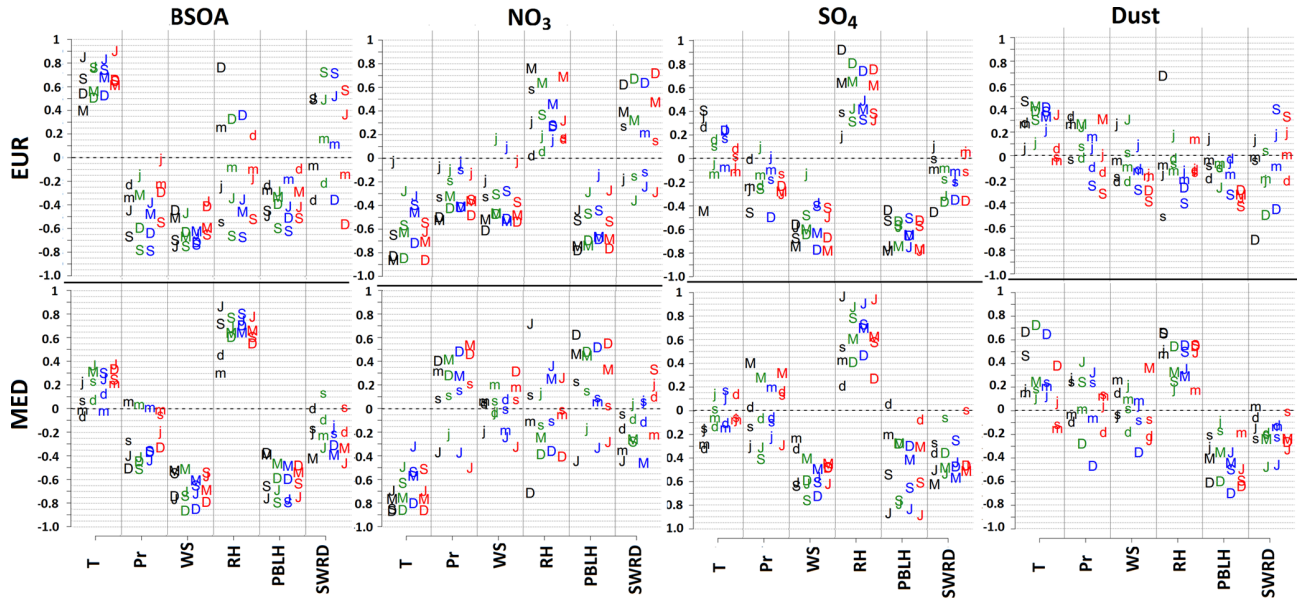


**Figure 10.** Correlation coefficient between all meteorological parameters tested and BSOA, ($NO_3$), sulfate ($SO_4^{-2}$) and dust particles for all seasons and the EUR and MED subdomains. D, M, J and S represent winter, spring, summer and fall, respectively (first letter of the first month of each season). Uppercase letters mean that the correlation between the two parameters is statistically significant, whereas lowercase letters show the contrary. Color coding for different scenarios is the same as in previous figures.

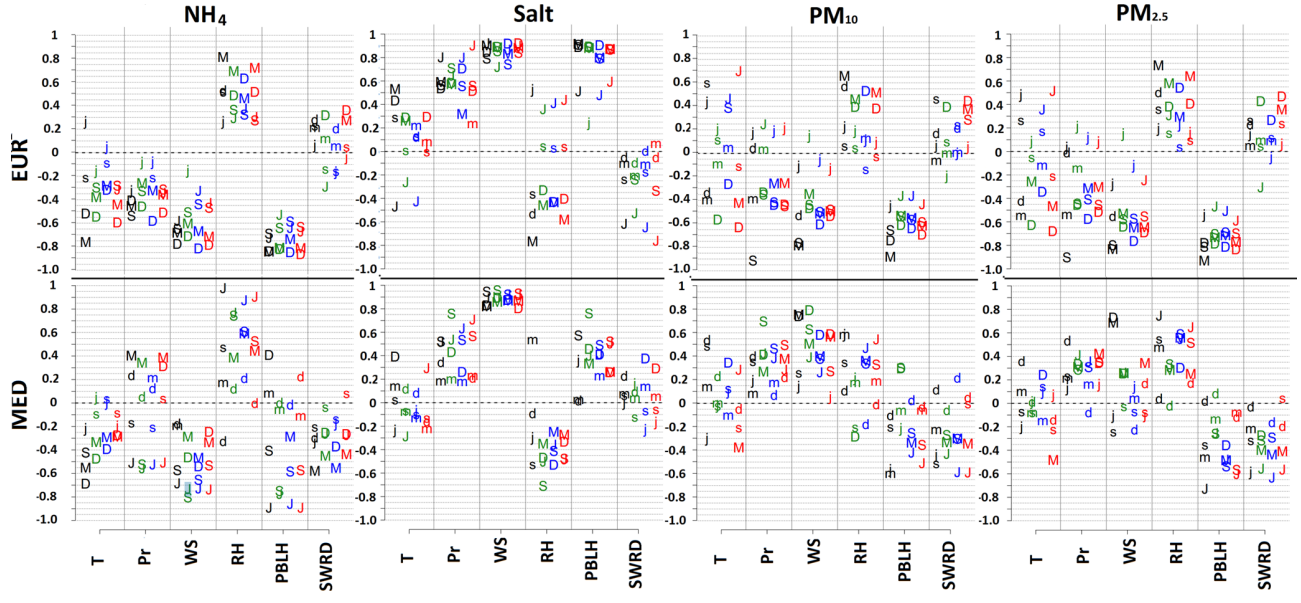


**Figure 11.** Correlation coefficient between all meteorological parameters tested and ammonium ($NH_4^+$), salt, $PM_{10}$ and $PM_{2.5}$ particles for all seasons and the EUR and MED subdomains. D, M, J and S represent winter, spring, summer and fall, respectively (first letter of the first month of each season). Uppercase letters mean that the correlation between the two parameters is statistically significant, whereas lowercase letters show the contrary. Color coding for different scenarios is the same as in previous figures. SWRD represents shortwave radiation.

correlation of wind speed with these two parameters. Another notable fact is the percentage of the concentration of BSOA that is formed from isoprene and monoterpenes; year-long sensitivity tests (with the reduction of respective terpene and isoprene emissions by 10 % in two separate 1-year-long simulations) for the year 1998 with historic climate show a distribution of 21 % and 79 % annually and 39 % and 61 % for the summer period for the concentration of BSOA forming from isoprene and monoterpenes, respectively. The isoprene to monoterpene emission ratio was 2.9 annually and

6.1 for the summer. Similar results were reported in Aksoyoglu et al. (2017).

### 3.4.3 Dust and salt particles

Dust concentrations are predicted to be at their maximum during spring (Fig. 9). This phenomena is also described in the literature for different regions (Werner et al., 2002, and Ginoux et al., 2004 explored global simulations; Laurent et al., 2005, focused on China and Mongolia; and Vincent et al., 2016, studied the western Mediterranean). In our simulations, the spatial maximum in dust particle concentrations normally occurs in the eastern Mediterranean (Figs. 8, 9, 10). While a decrease is observed for RCP4.5 and RCP8.5 (Fig. 7, for EUR $-5.6\,\%$ and $-5.3\,\%$, respectively), these particles do not exhibit any sensible variations in RCP2.6. As dust emissions are not taken into account within the simulated domain in our simulations and boundary conditions are the same in these scenarios, changes in the advection of dust aerosols is responsible for these variations. Therefore only advection plays a role, and cannot be captured by a local correlation analysis by definition.

The reason for the increase in dust particles in RCP2.6 scenarios for MEDE could be the different behavior that is seen in meteorological parameters for this subdomain compared with the others. The temperature decreases in this scenario after the 2040s in contrast with the other two scenarios, and therefore induces changes in RH that are different from the other scenarios. The average RH in RCP2.6 remains higher than the other scenarios, although it is lower than historic simulations for MEDE (Fig. S9). Until this point, we mostly have discussed climate change related modifications in PM sources, some sinks and transport. However, we should also take the effect of climate related changes effecting wet deposition into account. For RCP4.5 and RCP8.5, the amount of precipitation remains rather constant over the MEDW, whereas it increases in RCP2.6 (Fig. S3). The precipitation duration decreases for RCP4.5 and RCP8.5 over this subdomain, whereas it stays quite constant for RCP2.6 for MEDW. Thus, both the amount of precipitation and the precipitation duration are stronger in RCP2.6 than in RCP4.5 or RCP8.5. This could, in addition to different advection patterns, explain the lower MEDW dust concentrations in RCP2.6. However, for MEDE, the amount of precipitation increases as the number of rainy hours decreases; this infers strong but infrequent rain episodes, which would explain the increase in the dust concentration in this subdomain. The impact of changing precipitation frequency/amount is the dominant factor in our simulations when it comes to dust concentration changes, as changes in precipitation patterns result in changes in the amount of wet deposition.

Salt particles show a high concentration in the Mediterranean area and also over the Atlantic Ocean; they are the most important PM species for the EUR and MED subdomains. Sea-salt emissions are very sensitive to wind speed, leading to a correlation between salt concentrations and wind speed (Fig. 11). Therefore, small changes in the salt concentration in future scenarios compared with historic simulations are mostly due to small wind speed changes in future climate.

### 3.4.4 Total $PM_{10}$ and $PM_{2.5}$ dependencies on meteorological components

Investigating the correlation between $PM_{10}$ and $PM_{2.5}$ and different meteorological parameters, reveals high spatial and temporal variability. For the EUR subdomain, for both $PM_{10}$ and $PM_{2.5}$ the PBLH parameter shows the highest correlation (anti-correlation). For the Mediterranean region, among all of the meteorological parameters investigated, $PM_{10}$ seems to be more affected by wind speed, whereas $PM_{2.5}$ seems to be more affected by more by RH. The analysis of the link between total $PM_{10}$ and total $PM_{2.5}$ with meteorological parameters (Fig. 11) is far less conclusive compared with the individual component analysis. As a generalized conclusion, $PM_{10}$ and $PM_{2.5}$ tend to follow the correlations of their largest contributor.

Finally, precipitation has been pointed out as a crucial, but difficult to model/predict parameter in both current and future meteorological/climatic simulations (Dale et al., 2001). In our study, the correlations of PM or PM components with the amount of annual precipitation are generally weak (and positive correlations are sometimes even seen instead of the expected anti-correlations). It has also been discussed, that total annual precipitation duration could be more impactful on the PM than the total amount of precipitation (Dale et al., 2001). No correlation study was performed with this parameter in this work, but the decreasing total precipitation duration in all scenarios could induce some increase in PM and its components.

## 4 Impacts of boundary condition and anthropogenic emissions

While climate on its own can have important impacts on the future concentrations of different species, other drivers might have their specific effects on PM concentrations, which can either amplify or compensate for the climate-related effects. This section explores the impacts of two other drivers: boundary conditions and anthropogenic emissions. Five sets of simulations were used to achieve this goal, one where boundary conditions were changed together with climate inputs, and two where anthropogenic emissions were changed alongside climate inputs; these simulations were compared with historic simulations as well as climate simulations with constant boundary conditions and anthropogenic emissions. It should be noted that boundary conditions are taken from a global chemistry transport model; therefore, changing the boundary conditions corresponds to changing the global climate and the global anthropogenic emissions at the same

time. However, comparison between the regional climate change and the BC impact are strong enough for all compounds (see below) to conclude on a major driver, very probably beyond uncertainty. Finally, in an effort to provide a more comprehensive view of what the accumulative effects of all drivers would be, the aforementioned simulations are compared with a series of simulations where all drivers change at the same time. Keep in mind that the series of simulations where all drivers change at the same time show not only the accumulative impacts of all drivers, but also the nonlinear relationships that exist between different drivers. In these simulations, RCP4.5 related climate and boundary conditions are compared with the historic ones, 2050 regional current legislations emissions (CLE) and maximum feasible reductions (MRF) are compared against 2010 emissions. In total, in this section, six series of simulations are presented (the numbers in parenthesis refer to Table 1): historic simulation (simulation 1), climate impact simulation (simulation 3), boundary condition impact (simulation 5), emission impact (simulations 6–7) and accumulative impacts (simulation 8). For each series, 10-year-long simulations are used, between 2046 and 2055 for future scenarios and between 1996 and 2005 for historic simulations. In this way, the effect of boundary conditions, emissions and climate are calculated separately and compared with the overall changes in simulation 8. In Fig. 12 the impact of each driver is shown separately in terms of relative change (Sect. S8 for seasonal changes).

### 4.1 Boundary conditions

Among $PM_{10}$ components, dust, nitrate, BSOA, POA and sulfates show the highest impact on future PM concentrations when boundary conditions change, with other species showing only minor changes or no change at all (Fig. 12). Among these species, dust particles show the strongest dependence on boundary conditions: an increase of $+77 \pm 2\,\%$, $+30 \pm 10.7\,\%$, $+9 \pm 1.9\,\%$ and $+51 \pm 15.2\,\%$ for EUR, MED, MEDW and MEDE, respectively, for future RCP4.5 with respect to historic boundary conditions. Their simulated dependence on regional climate was indeed much smaller ($-9 \pm 0.3\,\%$, $-4 \pm 1.4\,\%$, $+3 \pm 0.6\,\%$ and $-4 \pm 1.8\,\%$ for EUR, MED, MEDW and MEDE, respectively, for the same period). It is important to bear in mind that the concentration of dusts in the European subdomain in our simulations is $0.8\,\mu g\,m^{-3}$ on average with an important spatial variability, with concentrations dropping significantly as we move further north (Fig. 9). Therefore, the low relative changes simulated for the Mediterranean subdomains have to be considered as a sign of the high absolute sensitivity to the scenario. The reason for the important changes in these species may be due to wind intensity and humidity in source regions or land use changes caused by climate change outside our domain. There are many uncertainties regarding the future changes of dust concentrations (Tegen et al., 2004; Woodward et al., 2005). Changes in climate drivers such as precipitation, wind speed, regional moisture balance in source areas, and land use changes, either resulting from anthropogenic changes or for climatic reasons, can have important effects on dust emissions (Harrison et al., 2001). Projection of changes in land use resulting from both sources are highly uncertain, which results in strong uncertainties in the projections of dust concentration changes in future scenarios (Tegen et al., 2004; Evan et al., 2014). Furthermore, the Mediterranean Sea is located on the southern border of the domain used in this study; therefore, it should be noted that although the results of dust concentration changes seen in this study are consistent with existing literature, the model might not be capable of consistently capturing the relationship between boundary condition changes and the southern parts of the Mediterranean due to the position of the domain. This is not the case for the European subdomain.

Nitrates and BSOA are more affected by climate change impacts than by boundary condition input changes in all subdomains ($-13 \pm 2.6\,\%$, $+14 \pm 0.5\,\%$, $-2 \pm 0.8\,\%$ and $+12 \pm 0.7\,\%$ for RCP4.5 compared with $-6 \pm 2.5\,\%$, $-26 \pm 0.5\,\%$, $-23 \pm 0.9\,\%$ and $-25 \pm 0.7\,\%$ for boundary condition changes for nitrates and $+12 \pm 1.3\,\%$, $+23 \pm 1\,\%$, $+24 \pm 1\,\%$ and $+12 \pm 1.1\,\%$ for RCP4.5 compared with $+6 \pm 1.3\,\%$, $+14 \pm 1.3\,\%$, $+7 \pm 1\,\%$ and $+14 \pm 1.4\,\%$ for BSOA for EUR, MED, MEDW and MEDE, respectively).

Contrary to the species discussed above, sulfates and POA are more sensitive to boundary conditions than to climate effects. Sulfates show a $-2 \pm 1.2\,\%$, $-7 \pm 1.6\,\%$, $-6 \pm 0.9\,\%$ and $-7 \pm 1\,\%$ decrease, whereas POA shows a $-9 \pm 0.7\,\%$, $-26 \pm 0.1\,\%$, $-11 \pm 0.1\,\%$ and $-19 \pm 0.1\,\%$ decrease related to boundary conditions for EUR, MED, MEDW and MEDE, respectively. Climate effects on these particles were smaller.

Ammonium shows a negligible change with regards to boundary conditions in EUR, and an increase in most Mediterranean subdomains ($+12 \pm 0.3\,\%$, $-1 \pm 0.1\,\%$ and $+12 \pm 0.2\,\%$ for MED, MEDW and MEDE), whereas the change in this species was mostly negative for climate impact results.

### 4.2 Anthropogenic emissions

Changes in anthropogenic emissions in CLE and MFR 2050 inputs are compared with CLE 2010 emissions for different species in the Supplement (Fig. S11). As expected, a decrease is seen for most species in CLE 2050 emissions, but to a higher extent in the MFR 2050 scenario. A simple comparison between CLE and MFR 2050 emission scenarios is shown in Fig. 13. Bear in mind that this figure shows the effects of climate change (RCP4.5) and emission change at the same time, as does every value presented in this paragraph. For CLE simulations, sulfates show a decrease of $-28 \pm 1.2\,\%$, $-29 \pm 1.3\,\%$, $-34 \pm 0.9\,\%$ and $-18 \pm 0.9\,\%$ for EUR, MED, MEDW and MEDE, respectively, with respect to historic simulations, whereas MFR scenarios show

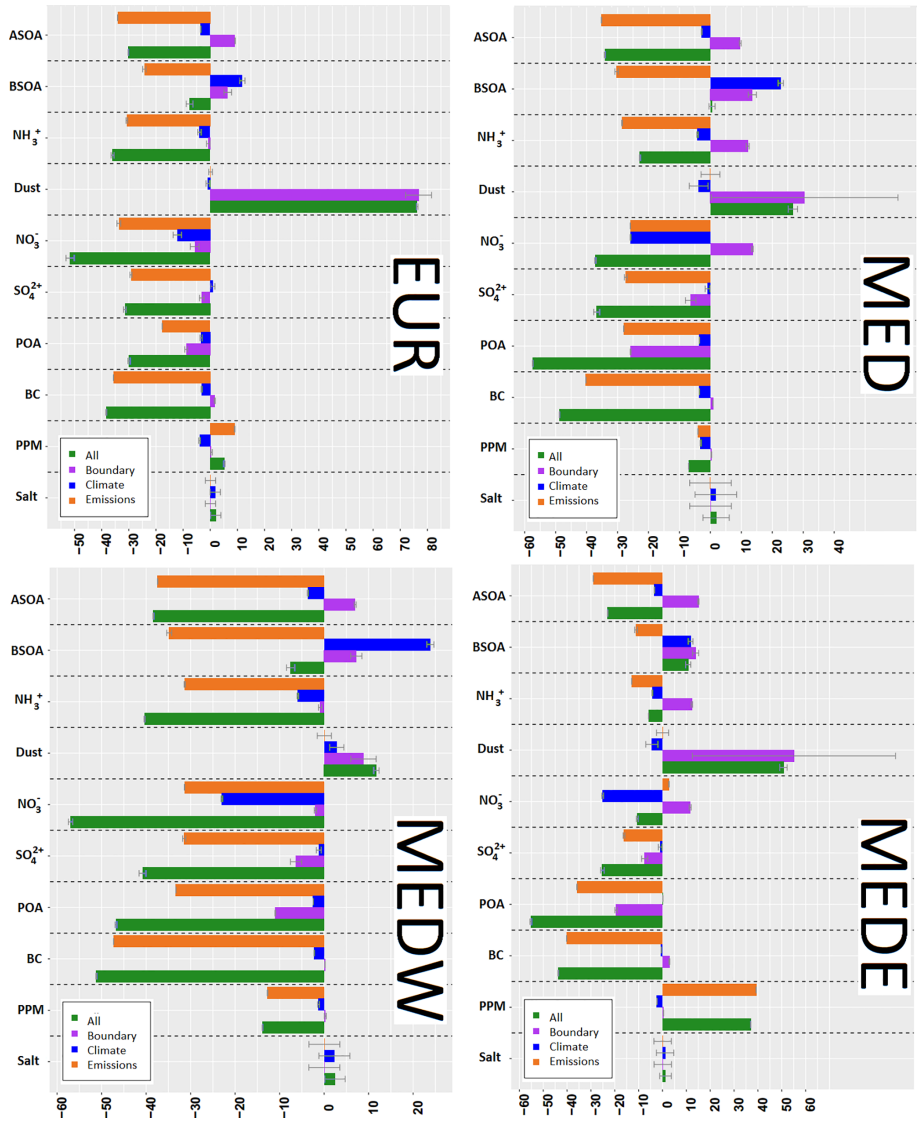


**Figure 12.** Relative impact of climate, boundary conditions and emission drivers on $PM_{10}$ components for different subdomains. Error bars show the confidence interval calculated on annual averages.

a $-60 \pm 1\,\%$, $-51 \pm 1.1\,\%$, $-55 \pm 0.8\,\%$ and $-52 \pm 0.7\,\%$ decrease for the same order of subdomains. The reason for this decrease is the decrease in the emissions of $SO_2$ ($SO_2$ emissions reduction of $-30\,\%$, $-53\,\%$, $-52\,\%$ and $-42\,\%$ for CLE and $-60\,\%$, $-53\,\%$, $-57\,\%$ and $-68\,\%$ for MFR for the same order of subdomains). Particulate nitrates also show a strong decrease with the decrease of precursor emissions, presenting $-48 \pm 2.5\,\%$, $-32 \pm 0.4\,\%$, $-36 \pm 0.8\,\%$ and $-28 \pm 0.6\,\%$ for CLE and $-79 \pm 2.2\,\%$, $-61 \pm 0.4\,\%$, $-74 \pm 0.8\,\%$ and $-77 \pm 0.5\,\%$ for MFR for EUR, MED, MEDW and MEDE, respectively, ($NO_x$ emission reduction of $-60\,\%$, $-38\,\%$, $-48\,\%$ and $-30\,\%$ for CLE and $-84\,\%$, $-38\,\%$, $-76\,\%$ and $-76\,\%$ for MFR for the same order of subdomains). Ammonium displays the same behavior, showing $-36 \pm 1\,\%$, $-55 \pm 0.2\,\%$, $-56 \pm 0.1\,\%$ and $-18 \pm 0.1\,\%$ for CLE and $-68 \pm 0.9\,\%$, $-87 \pm 0.2\,\%$, $-87 \pm 0.1\,\%$ and $-64 \pm 0.1\,\%$ for MFR for EUR, MED, MEDW and MEDE, respectively. Other components such as BC and POA show a strong decrease, as their concentrations depend directly on the amount of anthropogenic emissions. Interestingly, BSOA concentrations also show a strong decrease related to changes in anthropogenic emissions (contrary to the increase for climate change alone). Values of $-7 \pm 1.3\,\%$, $-34 \pm 1.1\,\%$, $-39 \pm 1.1\,\%$ and $+4 \pm 1.3\,\%$ for CLE and $-36 \pm 1.1\,\%$, $-64 \pm 1\,\%$, $-65 \pm 0.9\,\%$ and $-35 \pm 1.1\,\%$ for MFR for EUR, MED, MEDW and MEDE are seen, respectively, for this species. The fact that the decrease in anthropogenic emissions overshadows the increase in BSOA when looking at climate and boundary condition effects is an important message to take away from these simulations. The exact mechanism

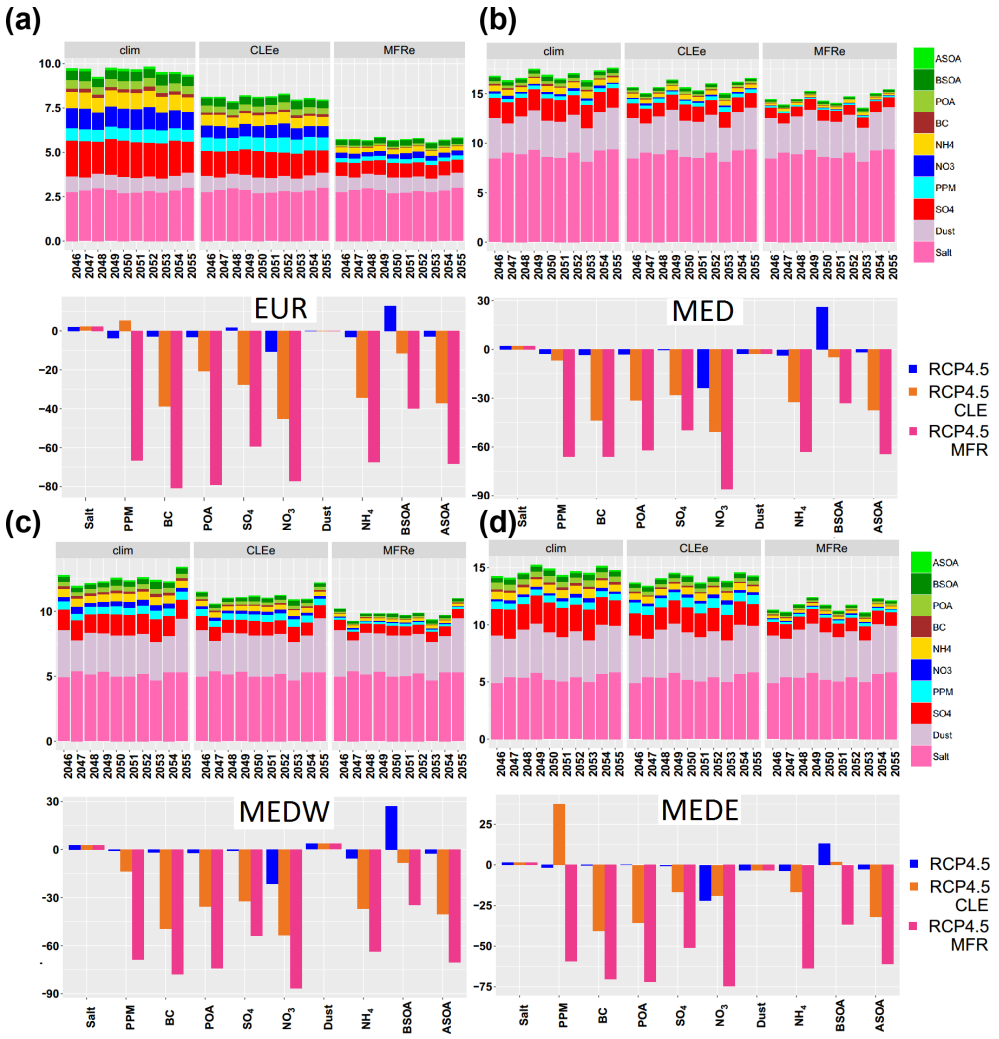


**Figure 13.** Emission scenario comparisons. Each panel shows one subdomain, the upper subpanels show the $PM_{10}$ components for each scenario, the lower subpanels shows the percentage difference for each scenario ((future − historic)/historic · 100).

for this effect is not clear, although it could be due to the general decrease of seed aerosol in these scenarios modifying the gas–particle equilibrium for SVOCs formed from monoterpenes and isoprene oxidation. Changes in oxidant levels due to a decrease in anthropogenic emissions in addition to a direct decrease in anthropogenic VOCs may be other reasons for this change (i.e., less organic aerosol mass available for oxidation products to condense on).

For the comparison of driver impacts (Fig. 12), only CLE 2050 simulations for emission impact scenarios are used, as CLE 2050 emissions are used in the simulation where all drivers change (presented in Sect. 4.3). Almost all species show strong dependence on emission changes, except dust and salt particles. Quantitative effects vary for the Mediterranean subdomains: the effect of emission changes becomes less pronounced for species without maritime emission sources (such as $NH_4^+$), whereas they stay high for species like POA, BC and $SO_4^{2-}$ which can be emitted by shipping lines.

### 4.3 Cumulative impacts

To provide a more complete view of probable atmospheric composition (under the hypotheses of the scenario) in the 2050s, the "All" scenario (Fig. 12) shows the combined effects of all drivers changing at the same time. There are many uncertainties affecting future scenarios as can be surmised; however, with regard to drivers that are explored here, this scenario shows what a more realistic future air composition might look like. As seen in Fig. 12, and with regard to total $PM_{10}$ and $PM_{10}$ components, the changes in emissions set the tone for the future, meaning that a reduction in anthropogenic emissions overshadows the climate and the boundary condition drivers for most of species. This highlights that mitigating air pollution with respect to air quality in the fu-

ture depends greatly on the reduction of anthropogenic emissions.

For $PM_{10}$ for the period from 2046 to 2055 using RCP4.5, the different drivers indicate a decrease of −15.6 %, −6.7 %, −10.5 % and +4 % for EUR, MED, MEDW and MEDE, respectively, mainly driven by anthropogenic emissions. Due to the boundary condition changes, PM increases of +5.3 %, +6.8 %, +1.2 % and +15.1 % for EUR, MED, MEDW and MEDE, respectively, are observed, mainly because of the dust concentration increase. The climate impacts on $PM_{10}$ concentrations for the same period are −2.9 %, −0.5 %, +0.6 % and −1.6 % for EUR, MED, MEDW and MEDE, respectively. The total change for the period from 2046 to 2055 using RCP4.5 (meaning in simulations where all drivers change at the same time) is a decrease which is seen for all subdomains for $PM_{10}$ (−11.8 %, −1 % and −9.2 % for EUR, MED MEDW, and MEDE, respectively) except for MEDE where an increase of +9.1 % is observed. Thus, for most of the domains, the effect of emission reductions on $PM_{10}$ concentrations around 2050 is reduced to a certain extent by modifications of boundary conditions and regional climate.

## 5 Conclusion and discussion

We investigated the effect of different drivers on total $PM_{10}$ and $PM_{10}$ components in future scenarios for different subdomains. For this purpose, an exhaustive number of scenarios plus historic simulations were performed. The drivers that were taken into account included climate change, anthropogenic emissions and boundary condition changes. For each driver, simulations were compared against historic simulations and then the effect of a specific factor was calculated separately and compared with a scenario where all drivers changed at the same time. This approach was chosen as, in the existing climate change literature, the effects of different drivers are taken into account either all at once (Lacressonnière et al., 2017), separately but for a single driver and for a short period of time, separately but using sensitivity tests (Dawson et al., 2007; Megaritis et al., 2014), or in the best of cases, separately and for an acceptable period of time but for only one driver (Lemaire et al., 2016). The goal of this work was to explore multiple drivers separately for $PM_{10}$ and its components for a coherent and comparable set of future scenarios, thereby making climate change analysis more comprehensible and more easily finding the drivers with the most impact on the $PM_{10}$ future concentration changes. This work focuses on the Mediterranean area as well as the European region, as to date not many studies have focused on the climate change drivers in the Mediterranean area, although this region might be highly sensitive to climate change; therefore, this study directly responds to one of the major goals of the ChArMEx project, in the context of which the research was performed.

Future scenarios that we performed show that in the 2050s, in the case of an RCP4.5 scenario and CLE 2050 emissions, a general increase in temperature and a decrease of the total average $PM_{10}$ concentration is seen both in the European subdomain (−12 %) and the Mediterranean subdomain (−1 %). The diminution of $PM_{10}$ has also been reported in the literature for the European subdomain (e.g., Markakis et al., 2014; Lacressonnière et al., 2014, 2017): the intensity of this decrease changes with the period that is taken into account and the inputs used. The PM changes are far from uniform for different seasons. For the European area a maximum change of −24 % for spring and +9 % for summer is seen, whereas for the Mediterranean area a maximum change of +25 % for winter and −19 % for spring is observed. These values seem to indicate different behaviors in the Mediterranean and European areas. The reasons for these changes were explored driver by driver and the effect of each driver was estimated.

Regional climate change alone results in a decrease of $PM_{10}$ in RCP4.5 and RCP8.5, whereas RCP2.6 shows an increase for $PM_{10}$. Among the $PM_{10}$ components, BSOA and nitrate particles show the most sensitivity to climate change. It appears that, when exploring the impacts of climate change, nitrate decrease governs the decrease of $PM_{10}$ and $PM_{2.5}$ in RCP4.5 and RCP8.5; however, in RCP2.6, the increase in dust, salt and BSOA particles outweighs the decrease in nitrates. In the search for reasons for the changes seen for PM components, correlations of meteorological parameters with individual components were investigated. Nitrates show a strong dependence (anti-correlation) on temperature, especially during winter, when a correlation with shortwave radiation and anti-correlations with wind speed and PBLH are also observed. These relationships seem to suggest a switch to slightly more "marine-type" conditions for a future climate during winter (supported by correlations calculated between different meteorological parameters). BSOA also shows a strong correlation with temperature (and therefore shows a strong increase in future scenarios) in all subdomains, resulting from an increase in BVOC emissions due to higher temperatures. Sulfate particles are seen to have a correlation with RH and PBLH, although the extent of this correlation changes depending on the subdomain explored. The relationship of $SO_4^{2-}$ with RH can be related to either the production of this aerosol from $SO_2$ or the formation of gas-phase $SO_4^{2-}$ from the oxidation of $SO_2$ by OH; the dominance of these processes depends on the subdomain and the season in which they are studied. Because of the general RH pattern differences between RCP2.6 compared with RCP4.5 and RCP8.5, sulfates show a particular 2-D structure in RCP2.6, which is different from the general pattern seen for RCP4.5 and RCP8.5. The relationship of ammonium aerosols with meteorological conditions is a combination of the relationships of $SO_4^{2-}$ and $NO_3^-$ with these conditions. Salt particles show a clear correlation with wind speed, whereas dust concentrations present a weak relationship with the meteorological parameters tested, as their changes are re-

lated to advection from outside the model domain and are, therefore, not captured by local correlation analysis.

Future changes in boundary conditions (depicting long-range transport from outside of Europe) greatly affect dust concentrations, especially over the Mediterranean area. In contrast, they only have a limited impact on sulfate, nitrate, ammonium and OA concentrations. It is important to keep in mind that, because of the position of the EURO-CORDEX domain and the fact that the southern part of the Mediterranean is located at the southern borders of the domain, the model might not be able to capture the effects of global climate change and dust activity in a fully consistent way, although the results show an important increase in dust concentrations due to long-range transport.

Emission changes show the largest effect on all non-sea-salt and non-dust $PM_{10}$/$PM_{2.5}$ components. One of the most interesting cases that was encountered in the emission change scenarios was the decrease in BSOA due to anthropogenic emission changes. This is tentatively attributed to changes in seed aerosol and the changes in oxidant levels because of the decrease in anthropogenic emissions in addition to a direct decrease in anthropogenic COVs. The same impact, with the same important intensity, was seen in a study in preparation by Ciarelli et al. (2019), when looking at an ensemble of simulations in the framework of the EURODELTA multi-model experiment. Sartelet et al. (2012) also noted an important change in SOA concentration in their simulation when changing the anthropogenic emissions. However, the exact mechanism of this relationship still needs further investigation. Compared with the other two drivers, the effects shown by the anthropogenic emission reduction are undeniably more important for most species. This leads us to the conclusion that, according to our study, anthropogenic emission reduction policies (or the lack thereof) will have a strong impact on the concentrations of PM seen in the future; furthermore, the impact of anthropogenic emissions will be more significant than the affects of both regional climate and long-range transport.

Another point that has been raised in this article is the differences between the European subdomain and the Mediterranean Sea and the difference between the eastern and western Mediterranean. The behavior of these subdomains differs when they are exposed to climate change. Meteorological changes in the domain show increasing temperatures, increasing PBLH and decreasing humidity. Winters and springs seem to become drier, while the other two seasons become wetter with respect to the amount of precipitation; rain episodes also become more intense and shorter in most cases (except for RCP2.6). The concentration of $PM_{10}$ is generally higher in the Mediterranean due to higher concentrations of dust and salt particles, whereas its annually averaged changes in the future remain quite similar to what was seen for the European subdomain. Seasonally, in the Mediterranean a maximum for $PM_{10}$ concentrations is seen for spring when dust episodes are more common, contrary to the European subdomain (maximum in winter for EUR). Emission reduction policies will reduce the concentrations of anthropogenic species in the basin by almost the same percentage as the European subdomain shown in this work (for example, for sulfates, anthropogenic emissions reduction results in $-29\,\%$ and $-30\,\%$ for EUR and MED, respectively, for CLE2050 emissions). While this fact shows that emission reduction policies will reduce the $PM_{2.5}$ and lower the aerosol fraction of pollution, they will not lessen the Mediterranean $PM_{10}$ burden by much, as the $PM_{10}$ concentration in this area is dominated by dust and salt concentrations. For the dust concentrations, our scenarios show an increased concentration in the Mediterranean due to long-range transport, especially in the eastern basin. However, changing land use in the northern African area will affect the concentration of dust in the Mediterranean; however, the extent and even the direction of this change is uncertain. Literature suggests that the dust concentrations due to land use changes in future scenarios can decrease or increase depending on the scenario that has been taken into account (Tegen et al., 2004; Woodward et al., 2005).

While exploring the three aforementioned drivers is important for understanding the behavior of PM and PM components in the future, there are other aspects that also need exploring in future studies. Other additions to this study would be, for example, to explore the effects of land use changes, OA simulation scheme changes and BSOA trend changes related to ASOA changes. Land use changes, apart from the previously mentioned effects on dust emission, can affect the emissions of BVOC, which can change the future concentrations of BSOA and can also change the deposition of different species in future scenarios. Additions to inorganic aerosol formation in future scenarios (such as different salt formation schemes, dimethyl sulfide formation from the sea surface and so on) would also be useful additions to the field of climate change study. Furthermore, the driver by driver approach can be taken with each of these parameters in order to explore their effects on future changes of PM concentrations.

*Data availability.* Access to the data used in this article is restricted to registered users of the ChArMEx project. The data are available from the project website (http://mistrals.sedoo.fr/ChArMEx/, last access: 15 July 2019) and should be used following the data and publication policies of the ChArMEx project: http://mistrals.sedoo.fr/ChArMEx/Data-Policy/ChArMEx_DataPolicy.pdf (last access: 7 August 2018).

*Supplement.* The supplement related to this article is available online at: https://doi.org/10.5194/acp-19-4459-2019-supplement.

*Author contributions.* ArC, AuC and MB designed the experiment. AuC performed the simulations, and ArC carried out the post-processing of aforementioned simulations. Article reduction was performed by ArC, and all authors contributed to the text, interpretation of the results and review of the article.

*Competing interests.* The authors declare that they have no conflict of interest.

*Special issue statement.* This article is part of the special issue "CHemistry and AeRosols Mediterranean EXperiments (ChArMEx) (ACP/AMT inter-journal SI)". It is not associated with a conference.

*Acknowledgements.* This research received funding from the French National Research Agency (ANR) projects SAF-MED (grant no. ANR-15 12-BS06-0013). This work is part of the ChArMEx project supported by ADEME, CEA, CNRS-INSU and Météo-France through the multidisciplinary MISTRALS (Mediterranean Integrated Studies aT Regional And Local Scales) program. The work presented here received support from the French Ministry in charge of ecology. This work was performed using HPC resources from GENCI-CCRT (grant no. 2017-t2015017232). Robert Vautard is acknowledged for providing the WRF/IPSL-CM5-MR Cordex simulations, and Didier Hauglustaine and Sophie Szopa are acknowledged for providing the INCA simulations. Zbigniew Klimont is acknowledged for providing the ECLIPSE-v4 emission projections. The thesis work of Arineh Cholakian is supported by ADEME, INERIS (with the support of the French Ministry in charge of Ecology), and via the ANR SAF-MED project. Giancarlo Ciarelli thanks ADEME and the Swiss National Science Foundation (grant no. P2EZP2_175166).

*Review statement.* This paper was edited by Jean-Luc Attié and reviewed by three anonymous referees.

## References

Aksoyoglu, S., Ciarelli, G., El-Haddad, I., Baltensperger, U., and Prévôt, A. S. H.: Secondary inorganic aerosols in Europe: sources and the significant influence of biogenic VOC emissions, especially on ammonium nitrate, Atmos. Chem. Phys., 17, 7757–7773, https://doi.org/10.5194/acp-17-7757-2017, 2017.

Amann, M., Klimont, Z., and Wagner, F.: Regional and Global Emissions of Air Pollutants: Recent Trends and Future Scenarios, Annu. Rev. Env. Resour., 38, 31–55, https://doi.org/10.1146/annurev-environ-052912-173303, 2013.

Anderson, J. O., Thundiyil, J. G., and Stolbach, A.: Clearing the Air: A Review of the Effects of Particulate Matter Air Pollution on Human Health, J. Med. Toxicol., 8, 166–175, https://doi.org/10.1007/s13181-011-0203-1, 2012.

Arino, O., Bicheron, P., Achard, F., Latham, J., Witt, R., and Weber, J.: Globcover: The most detailed protrait of Earth, Eur. Sp. Agency Bull., 36, 24–31, 2008.

Arneth, A., Miller, P. A., Scholze, M., Hickler, T., Schurgers, G., Smith, B., and Prentice, I. C.: $CO_2$ inhibition of global terrestrial isoprene emissions: Potential implications for atmospheric chemistry, Geophys. Res. Lett., 34, L18813, https://doi.org/10.1029/2007GL030615, 2007.

Bessagnet, B., Menut, L., Curci, G., Hodzic, A., Guillaume, B., Liousse, C., Moukhtar, S., Pun, B., Seigneur, C., and Schulz, M.: Regional modeling of carbonaceous aerosols over Europe – focus on secondary organic aerosols, J. Atmos. Chem., 61, 175–202, https://doi.org/10.1007/s10874-009-9129-2, 2008.

Carvalho, A., Monteiro, A., Solman, S., Miranda, A. I., and Borrego, C.: Climate-driven changes in air quality over Europe by the end of the 21st century, with special reference to Portugal, Environ. Sci. Policy, 13, 445–458, https://doi.org/10.1016/J.ENVSCI.2010.05.001, 2010.

Ciarelli, G., Theobald, M. R., Vivanco, M. G., Beekmann, M., Aas, W., Andersson, C., Bergström, R., Manders-Groot, A., Couvidat, F., Mircea, M., Tsyro, S., Fagerli, H., Mar, K., Raffort, V., Roustan, Y., Pay, M.-T., Schaap, M., Kranenburg, R., Adani, M., Briganti, G., Cappelletti, A., D'Isidoro, M., Cuvelier, C., Cholakian, A., Bessagnet, B., Wind, P., and Colette, A.: Trends of inorganic and organic aerosols and precursor gases in Europe: insights from the EURODELTA multi-model experiment over the 1990–2010 period, Geosci. Model Dev. Discuss., https://doi.org/10.5194/gmd-2019-70, in review, 2019.

Cholakian, A., Beekmann, M., Colette, A., Coll, I., Siour, G., Sciare, J., Marchand, N., Couvidat, F., Pey, J., Gros, V., Sauvage, S., Michoud, V., Sellegri, K., Colomb, A., Sartelet, K., Langley DeWitt, H., Elser, M., Prévot, A. S. H., Szidat, S., and Dulac, F.: Simulation of fine organic aerosols in the western Mediterranean area during the ChArMEx 2013 summer campaign, Atmos. Chem. Phys., 18, 7287–7312, https://doi.org/10.5194/acp-18-7287-2018, 2018.

Colette, A., Bessagnet, B., Vautard, R., Szopa, S., Rao, S., Schucht, S., Klimont, Z., Menut, L., Clain, G., Meleux, F., Curci, G., and Rouïl, L.: European atmosphere in 2050, a regional air quality and climate perspective under CMIP5 scenarios, Atmos. Chem. Phys., 13, 7451–7471, https://doi.org/10.5194/acp-13-7451-2013, 2013.

Colette, A., Andersson, C., Baklanov, A., Bessagnet, B., Brandt, J., Christensen, J. H., Doherty, R., Engardt, M., Geels, C., Giannakopoulos, C., Hedegaard, G. B., Katragkou, E., Langner, J., Lei, H., Manders, A., Melas, D., Meleux, F., Rouïl, L., Sofiev, M., Soares, J., Stevenson, D. S., Tombrou-Tzella, M., Varotsos, K. V., and Young, P.: Is the ozone climate penalty robust in Europe?, Environ. Res. Lett., 10, 084015, https://doi.org/10.1088/1748-9326/10/8/084015, 2015.

Dale, V. H., Joyce, L. A., McNulty, S., Neilson, R. P., Ayres, M. P., Flannigan, M. D., Hanson, P. J., Irland, L. C., Lugo, A. E., Peterson, C. J., Simberloff, D., Swanson, F. J., Stocks, B. J., and Wotton, B. M.: Climate Change and Forest Disturbances: Climate change can affect forests by altering the frequency, intensity, duration, and timing of fire, drought, introduced species, insect and pathogen outbreaks, hurricanes, windstorms, ice storms, or landslides, Bioscience, 51, 723–734, https://doi.org/10.1641/0006-3568(2001)051[0723:ccafd]2.0.co;2, 2001.

Dawson, J. P., Adams, P. J., and Pandis, S. N.: Sensitivity of $PM_{2.5}$ to climate in the Eastern US: a modeling case study, Atmos. Chem. Phys., 7, 4295-4309, https://doi.org/10.5194/acp-7-4295-2007, 2007.

de Winter, R. C., Sterl, A., and Ruessink, B. G.: Wind extremes in the North Sea Basin under climate change: An ensemble study of 12 CMIP5 GCMs, J. Geophys. Res.-Atmos., 118, 1601–1612, https://doi.org/10.1002/jgrd.50147, 2013.

Dobrynin, M., Murawsky, J., and Yang, S.: Evolution of the global wind wave climate in CMIP5 experiments, Geophys. Res. Lett., 39, L18606, https://doi.org/10.1029/2012GL052843, 2012.

Dufresne, J.-L., Foujols, M.-A., Denvil, S., Caubel, A., Marti, O., Aumont, O., Balkanski, Y., Bekki, S., Bellenger, H., Benshila, R., Bony, S., Bopp, L., Braconnot, P., Brockmann, P., Cadule, P., Cheruy, F., Codron, F., Cozic, A., Cugnet, D., de Noblet, N., Duvel, J.-P., Ethé, C., Fairhead, L., Fichefet, T., Flavoni, S., Friedlingstein, P., Grandpeix, J.-Y., Guez, L., Guilyardi, E., Hauglustaine, D., Hourdin, F., Idelkadi, A., Ghattas, J., Joussaume, S., Kageyama, M., Krinner, G., Labetoulle, S., Lahellec, A., Lefebvre, M.-P., Lefevre, F., Levy, C., Li, Z. X., Lloyd, J., Lott, F., Madec, G., Mancip, M., Marchand, M., Masson, S., Meurdesoif, Y., Mignot, J., Musat, I., Parouty, S., Polcher, J., Rio, C., Schulz, M., Swingedouw, D., Szopa, S., Talandier, C., Terray, P., Viovy, N., and Vuichard, N.: Climate change projections using the IPSL-CM5 Earth System Model: from CMIP3 to CMIP5, Clim. Dynam., 40, 2123–2165, https://doi.org/10.1007/s00382-012-1636-1, 2013.

EEA: Air pollution and climate change policies in Europe: exploring linkages and the added value of an integrated approach, European Environment Agency, Copenhagen, available at: https://www.eea.europa.eu/publications/technical_report_2004_5 (last access: 7 December 2017), 2004.

EEA: Air quality in Europe – 2016, European Environment Agency, Copenhagen, available at: https://www.eea.europa.eu//publications/air-quality-in-europe-2016 (last access: 11 December 2017), 2016.

Evan, A. T., Flamant, C., Fiedler, S., and Doherty, O.: An analysis of aeolian dust in climate models, Geophys. Res. Lett., 41, 5996–6001, https://doi.org/10.1002/2014GL060545, 2014.

Fichefet, T. and Maqueda, M. A. M.: Modelling the influence of snow accumulation and snow-ice formation on the seasonal cycle of the Antarctic sea-ice cover, Clim. Dynam., 15, 251–268, https://doi.org/10.1007/s003820050280, 1999.

Fiore, A. M., Naik, V., Spracklen, D. V., Steiner, A., Unger, N., Prather, M., Bergmann, D., Cameron-Smith, P. J., Cionni, I., Collins, W. J., Dalsøren, S., Eyring, V., Folberth, G. A., Ginoux, P., Horowitz, L. W., Josse, B., Lamarque, J.-F., MacKenzie, I. A., Nagashima, T., O'Connor, F. M., Righi, M., Rumbold, S. T., Shindell, D. T., Skeie, R. B., Sudo, K., Szopa, S., Takemura, T., and Zeng, G.: Global air quality and climate, Chem. Soc. Rev., 41, 6663, https://doi.org/10.1039/c2cs35095e, 2012.

Fortems-Cheiney, A., Foret, G., Siour, G., Vautard, R., Szopa, S., Dufour, G., Colette, A., Lacressonniere, G., and Beekmann, M.: A 3C global RCP8.5 emission trajectory cancels benefits of European emission reductions on air quality, Nat. Commun., 8, 89, https://doi.org/10.1038/s41467-017-00075-9, 2017.

Fountoukis, C. and Nenes, A.: ISORROPIA II: a computationally efficient thermodynamic equilibrium model for $K^+$-$Ca^{2+}$-$Mg^{2+}$-$NH_4^+$-$Na^+$-$SO_4^{2-}$-$NO_3^-$-$Cl^-$-$H_2O$ aerosols, Atmos. Chem. Phys., 7, 4639–4659, https://doi.org/10.5194/acp-7-4639-2007, 2007.

Ginoux, P., Prospero, J. M., Torres, O., and Chin, M.: Long-term simulation of global dust distribution with the GOCART model: correlation with North Atlantic Oscillation, Environ. Modell. Softw., 19, 113–128, https://doi.org/10.1016/S1364-8152(03)00114-2, 2004.

Giorgi, F.: Climate change hot-spots, Geophys. Res. Lett., 33, 1–4, https://doi.org/10.1029/2006GL025734, 2006.

Grantz, D., Garner, J. H., and Johnson, D.: Ecological effects of particulate matter, Environ. Int., 29, 213–239, https://doi.org/10.1016/S0160-4120(02)00181-2, 2003.

Guenther, A., Karl, T., Harley, P., Wiedinmyer, C., Palmer, P. I., and Geron, C.: Estimates of global terrestrial isoprene emissions using MEGAN (Model of Emissions of Gases and Aerosols from Nature), Atmos. Chem. Phys., 6, 3181–3210, https://doi.org/10.5194/acp-6-3181-2006, 2006.

Hantson, S., Knorr, W., Schurgers, G., Pugh, T. A. M., and Arneth, A.: Global isoprene and monoterpene emissions under changing climate, vegetation, $CO_2$ and land use, Atmos. Environ., 155, 35–45, https://doi.org/10.1016/j.atmosenv.2017.02.010, 2017.

Harrison, S. P., Kohfeld, K. E., Roelandt, C., and Claquin, T.: The role of dust in climate changes today, at the last glacial maximum and in the future, Earth-Sci. Rev., 54, 43–80, https://doi.org/10.1016/S0012-8252(01)00041-1, 2001.

Hauglustaine, D. A., Balkanski, Y., and Schulz, M.: A global model simulation of present and future nitrate aerosols and their direct radiative forcing of climate, Atmos. Chem. Phys., 14, 11031–11063, https://doi.org/10.5194/acp-14-11031-2014, 2014.

Heald, C. L., Henze, D. K., Horowitz, L. W., Feddema, J., Lamarque, J.-F., Guenther, A., Hess, P. G., Vitt, F., Seinfeld, J. H., Goldstein, A. H., and Fung, I.: Predicted change in global secondary organic aerosol concentrations in response to future climate, emissions, and land use change, J. Geophys. Res.-Atmos., 113, D05211, https://doi.org/10.1029/2007JD009092, 2008.

Hedegaard, G. B., Brandt, J., Christensen, J. H., Frohn, L. M., Geels, C., Hansen, K. M., and Stendel, M.: Impacts of Climate Change on Air Pollution Levels in the Northern Hemisphere with Special Focus on Europe and the Arctic, in: Air Pollution Modeling and Its Application XIX, 568–576, Springer Netherlands, Dordrecht, 2008.

Hedegaard, G. B., Christensen, J. H., and Brandt, J.: The relative importance of impacts from climate change vs. emissions change on air pollution levels in the 21st century, Atmos. Chem. Phys., 13, 3569–3585, https://doi.org/10.5194/acp-13-3569-2013, 2013.

Hodzic, A. and Jimenez, J. L.: Modeling anthropogenically controlled secondary organic aerosols in a megacity: a simplified framework for global and climate models, Geosci. Model Dev., 4, 901–917, https://doi.org/10.5194/gmd-4-901-2011, 2011.

Hourdin, F., Musat, I., Bony, S., Braconnot, P., Codron, F., Dufresne, J.-L., Fairhead, L., Filiberti, M.-A., Friedlingstein, P., Grandpeix, J.-Y., Krinner, G., LeVan, P., Li, Z.-X., and Lott, F.: The LMDZ4 general circulation model: climate performance and sensitivity to parametrized physics with emphasis on tropical convection, Clim. Dynam., 27, 787–813, https://doi.org/10.1007/s00382-006-0158-0, 2006.

Im, U., Brandt, J., Geels, C., Hansen, K. M., Christensen, J. H., Andersen, M. S., Solazzo, E., Kioutsioukis, I., Alyuz, U., Balzarini, A., Baro, R., Bellasio, R., Bianconi, R., Bieser, J.,

Colette, A., Curci, G., Farrow, A., Flemming, J., Fraser, A., Jimenez-Guerrero, P., Kitwiroon, N., Liang, C.-K., Nopmongcol, U., Pirovano, G., Pozzoli, L., Prank, M., Rose, R., Sokhi, R., Tuccella, P., Unal, A., Vivanco, M. G., West, J., Yarwood, G., Hogrefe, C., and Galmarini, S.: Assessment and economic valuation of air pollution impacts on human health over Europe and the United States as calculated by a multi-model ensemble in the framework of AQMEII3, Atmos. Chem. Phys., 18, 5967–5989, https://doi.org/10.5194/acp-18-5967-2018, 2018.

Jacob, D.: IMPACT2C – An introduction, Clim. Serv., 7, 1–2, https://doi.org/10.1016/J.CLISER.2017.07.006, 2017.

Jacob, D., Petersen, J., Eggert, B., Alias, A., Christensen, O. B., Bouwer, L. M., Braun, A., Colette, A., Déqué, M., Georgievski, G., Georgopoulou, E., Gobiet, A., Menut, L., Nikulin, G., Haensler, A., Hempelmann, N., Jones, C., Keuler, K., Kovats, S., Kröner, N., Kotlarski, S., Kriegsmann, A., Martin, E., van Meijgaard, E., Moseley, C., Pfeifer, S., Preuschmann, S., Radermacher, C., Radtke, K., Rechid, D., Rounsevell, M., Samuelsson, P., Somot, S., Soussana, J.-F., Teichmann, C., Valentini, R., Vautard, R., Weber, B., and Yiou, P.: EURO-CORDEX: new high-resolution climate change projections for European impact research, Reg. Environ. Change, 14, 563–578, https://doi.org/10.1007/s10113-013-0499-2, 2014.

Jacob, D. J. and Winner, D. A.: Effect of Climate Change on Air Quality, Atmos. Environ., 43, 51–63, https://doi.org/10.1016/j.atmosenv.2008.09.051, 2009.

Jiménez-Guerrero, P., Montávez, J. P., Gómez-Navarro, J. J., Jerez, S., and Lorente-Plazas, R.: Impacts of climate change on ground level gas-phase pollutants and aerosols in the Iberian Peninsula for the late XXI century, Atmos. Environ., 55, 483–495, https://doi.org/10.1016/j.atmosenv.2012.02.048, 2012.

Juda-Rezler, K., Reizer, M., Huszar, P., Krüger, B., Zanis, P., Syrakov, D., Katragkou, E., Trapp, W., Melas, D., Chervenkov, H., Tegoulias, I., and Halenka, T.: Modelling the effects of climate change on air quality over Central and Eastern Europe: concept, evaluation and projections, Clim. Res., 53, 179–203, https://doi.org/10.3354/cr01072, 2012.

Kampa, M. and Castanas, E.: Human health effects of air pollution, Environ. Pollut., 151, 362–367, https://doi.org/10.1016/J.ENVPOL.2007.06.012, 2008.

Katragkou, E., García-Díez, M., Vautard, R., Sobolowski, S., Zanis, P., Alexandri, G., Cardoso, R. M., Colette, A., Fernandez, J., Gobiet, A., Goergen, K., Karacostas, T., Knist, S., Mayer, S., Soares, P. M. M., Pytharoulis, I., Tegoulias, I., Tsikerdekis, A., and Jacob, D.: Regional climate hindcast simulations within EURO-CORDEX: evaluation of a WRF multi-physics ensemble, Geosci. Model Dev., 8, 603–618, https://doi.org/10.5194/gmd-8-603-2015, 2015.

Kerkhoff, C., Künsch, H. R., and Schär, C.: A Bayesian Hierarchical Model for Heterogeneous RCM–GCM Multimodel Ensembles, J. Climate, 28, 6249–6266, https://doi.org/10.1175/JCLI-D-14-00606.1, 2015.

Kinney, P. L.: Climate Change, Air Quality, and Human Health, Am. J. Prev. Med., 35, 459–467, https://doi.org/10.1016/j.amepre.2008.08.025, 2008.

Klimont, Z., Smith, S. J., and Cofala, J.: The last decade of global anthropogenic sulfur dioxide: 2000–2011 emissions, Environ. Res. Lett., 8, 014003, https://doi.org/10.1088/1748-9326/8/1/014003, 2013.

Klimont, Z., Kupiainen, K., Heyes, C., Purohit, P., Cofala, J., Rafaj, P., Borken-Kleefeld, J., and Schöpp, W.: Global anthropogenic emissions of particulate matter including black carbon, Atmos. Chem. Phys., 17, 8681–8723, https://doi.org/10.5194/acp-17-8681-2017, 2017.

Knutti, R. and Sedláček, J.: Robustness and uncertainties in the new CMIP5 climate model projections, Nat. Clim. Chang., 3, 369–373, https://doi.org/10.1038/NCLIMATE1716, 2012.

Kotlarski, S., Keuler, K., Christensen, O. B., Colette, A., Déqué, M., Gobiet, A., Goergen, K., Jacob, D., Lüthi, D., van Meijgaard, E., Nikulin, G., Schär, C., Teichmann, C., Vautard, R., Warrach-Sagi, K., and Wulfmeyer, V.: Regional climate modeling on European scales: a joint standard evaluation of the EURO-CORDEX RCM ensemble, Geosci. Model Dev., 7, 1297–1333, https://doi.org/10.5194/gmd-7-1297-2014, 2014.

Krinner, G., Viovy, N., de Noblet-Ducoudré, N., Ogée, J., Polcher, J., Friedlingstein, P., Ciais, P., Sitch, S., and Prentice, I. C.: A dynamic global vegetation model for studies of the coupled atmosphere-biosphere system, Global Biogeochem. Cy., 19, GB1015, https://doi.org/10.1029/2003GB002199, 2005.

Lacressonnière, G., Peuch, V.-H., Vautard, R., Arteta, J., Déqué, M., Joly, M., and Josse, B.: European air quality in the 2030s and 2050s: Impacts of global and regional emission trends and of climate change, Atmos. Environ., 92, 348–358, https://doi.org/10.1016/J.ATMOSENV.2014.04.033, 2014.

Lacressonnière, G., Foret, G., Beekmann, M., Siour, G., Engardt, M., Gauss, M., Watson, L., Andersson, C., Colette, A., Josse, B., Marécal, V., Nyiri, A., and Vautard, R.: Impacts of regional climate change on air quality projections and associated uncertainties, Climatic Change, 136, 309–324, https://doi.org/10.1007/s10584-016-1619-z, 2016.

Lacressonnière, G., Watson, L., Gauss, M., Magnuz, E., Andersson, C. B. M., Augustin, C., Gilles, F., Josse, B., Marécal, V., Nyiri, A., Siour, G., Sobolowski, S., and Vautard, R.: Particulate matter air pollution in Europe in a $+2\,^{\circ}C$ warming world, Atmos. Environ., 154, 129–140, https://doi.org/10.1016/J.ATMOSENV.2017.01.037, 2017.

Langner, J., Engardt, M., Baklanov, A., Christensen, J. H., Gauss, M., Geels, C., Hedegaard, G. B., Nuterman, R., Simpson, D., Soares, J., Sofiev, M., Wind, P., and Zakey, A.: A multi-model study of impacts of climate change on surface ozone in Europe, Atmos. Chem. Phys., 12, 10423–10440, https://doi.org/10.5194/acp-12-10423-2012, 2012.

Lathière, J., Hauglustaine, D. A., De Noblet-Ducoudré, N., Krinner, G., and Folberth, G. A.: Past and future changes in biogenic volatile organic compound emissions simulated with a global dynamic vegetation model, Geophys. Res. Lett., 32, L20818, https://doi.org/10.1029/2005GL024164, 2005.

Laurent, B., Marticorena, B., Bergametti, G., Chazette, P., Maignan, F., and Schmechtig, C.: Simulation of the mineral dust emission frequencies from desert areas of China and Mongolia using an aerodynamic roughness length map derived from the POLDER/ADEOS 1 surface products, J. Geophys. Res., 110, D18S04, https://doi.org/10.1029/2004JD005013, 2005.

Lemaire, V. E. P., Colette, A., and Menut, L.: Using statistical models to explore ensemble uncertainty in climate impact studies: the example of air pollution in Europe, Atmos. Chem. Phys., 16, 2559–2574, https://doi.org/10.5194/acp-16-2559-2016, 2016.

Liao, H., Chen, W.-T., and Seinfeld, J. H.: Role of climate change in global predictions of future tropospheric ozone and aerosols, J. Geophys. Res., 111, D12304, https://doi.org/10.1029/2005JD006852, 2006.

Madec, G. and Delecluse, P.: OPA 8.1 Ocean General Circulation Model Reference Manual, Inst. Pierre Simon Laplace des Sci. l'environnement Glob., available at: https://www.researchgate.net/profile/Gurvan_Madec/publication/243055542_OPA_81_Ocean_General_Circulation_Model_reference_manual/links/02e7e51d1b695c81c5000000/OPA-81-Ocean-General-Circulation-Model-reference-manual.pdf (last access: 26 January 2018), 1998.

Markakis, K., Valari, M., Colette, A., Sanchez, O., Perrussel, O., Honore, C., Vautard, R., Klimont, Z., and Rao, S.: Air quality in the mid-21st century for the city of Paris under two climate scenarios; from the regional to local scale, Atmos. Chem. Phys., 14, 7323–7340, https://doi.org/10.5194/acp-14-7323-2014, 2014.

Marticorena, B. and Bergametti, G.: Modeling the atmospheric dust cycle: 1. Design of a soil-derived dust emission scheme, J. Geophys. Res., 100, 16415, https://doi.org/10.1029/95JD00690, 1995.

Megaritis, A. G., Fountoukis, C., Charalampidis, P. E., Denier van der Gon, H. A. C., Pilinis, C., and Pandis, S. N.: Linking climate and air quality over Europe: effects of meteorology on $PM_{2.5}$ concentrations, Atmos. Chem. Phys., 14, 10283–10298, https://doi.org/10.5194/acp-14-10283-2014, 2014.

Meinshausen, M., Smith, S. J., Calvin, K., Daniel, J. S., Kainuma, M. L. T., Lamarque, J.-F., Matsumoto, K., Montzka, S. A., Raper, S. C. B., Riahi, K., Thomson, A., Velders, G. J. M., and van Vuuren, D. P. P.: The RCP greenhouse gas concentrations and their extensions from 1765 to 2300, Climatic Change, 109, 21–241, https://doi.org/10.1007/s10584-011-0156-z, 2011.

Meleux, F., Solmon, F., and Giorgi, F.: Increase in summer European ozone amounts due to climate change, Atmos. Environ., 41, 7577–7587, https://doi.org/10.1016/J.ATMOSENV.2007.05.048, 2007.

Menut, L., Tripathi, O. P., Colette, A., Vautard, R., Menut, L., Flaounas, E., Tripathi, O. P., Vautard, R., and Bessagnet, B.: Evaluation of regional climate simulations for air quality modelling purposes, Clim. Dynam., 40, 2515–2533, https://doi.org/10.1007/s00382-012-1345-9, 2012.

Menut, L., Bessagnet, B., Khvorostyanov, D., Beekmann, M., Blond, N., Colette, A., Coll, I., Curci, G., Foret, G., Hodzic, A., Mailler, S., Meleux, F., Monge, J.-L., Pison, I., Siour, G., Turquety, S., Valari, M., Vautard, R., and Vivanco, M. G.: CHIMERE 2013: a model for regional atmospheric composition modelling, Geosci. Model Dev., 6, 981–1028, https://doi.org/10.5194/gmd-6-981-2013, 2013.

Menut, L., Rea, G., Mailler, S., Khvorostyanov, D., and Turquety, S.: Aerosol forecast over the Mediterranean area during July 2013 (ADRIMED/CHARMEX), Atmos. Chem. Phys., 15, 7897–7911, https://doi.org/10.5194/acp-15-7897-2015, 2015.

Olesen, J. E., Carter, T. R., Díaz-Ambrona, C. H., Fronzek, S., Heidmann, T., Hickler, T., Holt, T., Minguez, M. I., Morales, P., Palutikof, J. P., Quemada, M., Ruiz-Ramos, M., Rubæk, G. H., Sau, F., Smith, B., and Sykes, M. T.: Uncertainties in projected impacts of climate change on European agriculture and terrestrial ecosystems based on scenarios from regional climate models, Climatic Change, 81, 123–143, https://doi.org/10.1007/s10584-006-9216-1, 2007.

Pacifico, F., Folberth, G. A., Jones, C. D., Harrison, S. P., and Collins, W. J.: Sensitivity of biogenic isoprene emissions to past, present, and future environmental conditions and implications for atmospheric chemistry, J. Geophys. Res.-Atmos., 117, D22302, https://doi.org/10.1029/2012JD018276, 2012.

Petetin, H., Beekmann, M., Sciare, J., Bressi, M., Rosso, A., Sanchez, O., and Ghersi, V.: A novel model evaluation approach focusing on local and advected contributions to urban $PM_{2.5}$ levels – application to Paris, France, Geosci. Model Dev., 7, 1483–1505, https://doi.org/10.5194/gmd-7-1483-2014, 2014.

Pope, C. A. and Dockery, D. W.: Health Effects of Fine Particulate Air Pollution: Lines that Connect, J. Air Waste Manage., 56, 709–742, https://doi.org/10.1080/10473289.2006.10464485, 2006.

Pope, C. A., Ezzati, M., and Dockery, D. W.: Fine-Particulate Air Pollution and Life Expectancy in the United States, N. Engl. J. Med., 360, 376–386, https://doi.org/10.1056/NEJMsa0805646, 2009.

Rea, G., Turquety, S., Menut, L., Briant, R., Mailler, S., and Siour, G.: Source contributions to 2012 summertime aerosols in the Euro-Mediterranean region, Atmos. Chem. Phys., 15, 8013–8036, https://doi.org/10.5194/acp-15-8013-2015, 2015.

Sartelet, K. N., Couvidat, F., Seigneur, C., and Roustan, Y.: Impact of biogenic emissions on air quality over Europe and North America, Atmos. Environ., 53, 131–141, https://doi.org/10.1016/J.ATMOSENV.2011.10.046, 2012.

Seinfeld, J. H. and Pandis, S. N.: Atmospheric chemistry and physics: from air pollution to climate change, John Wiley & Sons, 2016.

Shindell, D. T., Lamarque, J.-F., Schulz, M., Flanner, M., Jiao, C., Chin, M., Young, P. J., Lee, Y. H., Rotstayn, L., Mahowald, N., Milly, G., Faluvegi, G., Balkanski, Y., Collins, W. J., Conley, A. J., Dalsoren, S., Easter, R., Ghan, S., Horowitz, L., Liu, X., Myhre, G., Nagashima, T., Naik, V., Rumbold, S. T., Skeie, R., Sudo, K., Szopa, S., Takemura, T., Voulgarakis, A., Yoon, J.-H., and Lo, F.: Radiative forcing in the ACCMIP historical and future climate simulations, Atmos. Chem. Phys., 13, 2939–2974, https://doi.org/10.5194/acp-13-2939-2013, 2013.

Szopa, S., Hauglustaine, D. A., Vautard, R., and Menut, L.: Future global tropospheric ozone changes and impact on European air quality, Geophys. Res. Lett., 33, L14805, https://doi.org/10.1029/2006GL025860, 2006.

Szopa, S., Balkanski, Y., Schulz, M., Bekki, S., Cugnet, D., Fortems-Cheiney, A., Turquety, S., Cozic, A., Déandreis, C., Hauglustaine, D., Idelkadi, A., Lathière, J., Lefevre, F., Marchand, M., Vuolo, R., Yan, N., and Dufresne, J.-L.: Aerosol and ozone changes as forcing for climate evolution between 1850 and 2100, Clim. Dynam., 40, 2223–2250, https://doi.org/10.1007/s00382-012-1408-y, 2013.

Tai, A. P. K., Mickley, L. J., Heald, C. L., and Wu, S.: Effect of $CO_2$ inhibition on biogenic isoprene emission: Implications for air quality under 2000 to 2050 changes in climate, vegetation, and land use, Geophys. Res. Lett., 40, 3479–3483, https://doi.org/10.1002/grl.50650, 2013.

Taylor, K. E., Stouffer, R. J., Meehl, G. A., Taylor, K. E., Stouffer, R. J., and Meehl, G. A.: An Overview of CMIP5 and

the Experiment Design, B. Am. Meteorol. Soc., 93, 485–498, https://doi.org/10.1175/BAMS-D-11-00094.1, 2012.

Tegen, I., Werner, M., Harrison, S. P., and Kohfeld, K. E.: Relative importance of climate and land use in determining present and future global soil dust emission, Geophys. Res. Lett., 31, L05105, https://doi.org/10.1029/2003GL019216, 2004.

Teichmann, C., Eggert, B., Elizalde, A., Haensler, A., Jacob, D., Kumar, P., Moseley, C., Pfeifer, S., Rechid, D., Remedio, A., Ries, H., Petersen, J., Preuschmann, S., Raub, T., Saeed, F., Sieck, K., Weber, T., Teichmann, C., Eggert, B., Elizalde, A., Haensler, A., Jacob, D., Kumar, P., Moseley, C., Pfeifer, S., Rechid, D., Remedio, A. R., Ries, H., Petersen, J., Preuschmann, S., Raub, T., Saeed, F., Sieck, K., and Weber, T.: How Does a Regional Climate Model Modify the Projected Climate Change Signal of the Driving GCM: A Study over Different CORDEX Regions Using REMO, Atmosphere, 4, 214–236, https://doi.org/10.3390/atmos4020214, 2013.

Thomson, A. M., Calvin, K. V, Smith, S. J., Page Kyle, G., Volke, A., Patel, P., Delgado-Arias, S., Bond-Lamberty, B., Wise, M. A., Clarke, L. E., and Edmonds, J. A.: RCP4.5: a pathway for stabilization of radiative forcing by 2100, Climatic Change, 109, 77, https://doi.org/10.1007/s10584-011-0151-4, 2011.

Vautard, R., Gobiet, A., Sobolowski, S., Kjellström, E., Stegehuis, A., Watkiss, P., Mendlik, T., Landgren, O., Nikulin, G., Teichmann, C., and Jacob, D.: The European climate under a 2 °C global warming, Environ. Res. Lett., 9, 34006, https://doi.org/10.1088/1748-9326/9/3/034006, 2014.

Vautard, R., Colette, A., van Meijgaard, E., Meleux, F., Jan van Oldenborgh, G., Otto, F., Tobin, I., Yiou, P., Vautard, R., Colette, A., Meijgaard, E. van, Meleux, F., van Oldenborgh, G. J., Otto, F., Tobin, I., and Yiou, P.: Attribution of Wintertime Anticyclonic Stagnation Contributing to Air Pollution in Western Europe, B. Am. Meteorol. Soc., 99, S70–S75, https://doi.org/10.1175/BAMS-D-17-0113.1, 2018.

Vincent, J., Laurent, B., Losno, R., Bon Nguyen, E., Roullet, P., Sauvage, S., Chevaillier, S., Coddeville, P., Ouboulmane, N., di Sarra, A. G., Tovar-Sánchez, A., Sferlazzo, D., Massanet, A., Triquet, S., Morales Baquero, R., Fornier, M., Coursier, C., Desboeufs, K., Dulac, F., and Bergametti, G.: Variability of mineral dust deposition in the western Mediterranean basin and south-east of France, Atmos. Chem. Phys., 16, 8749–8766, https://doi.org/10.5194/acp-16-8749-2016, 2016.

van Vuuren, D. P., Stehfest, E., J den Elzen, M. G., Kram, T., van Vliet, J., Deetman, S., Isaac, M., Klein Goldewijk, K., Hof, A., Mendoza Beltran, A., Oostenrijk, R., and van Ruijven, B.: RCP2.6: exploring the possibility to keep global mean temperature increase below 2 °C, Climatic Change, 109, 95–116, https://doi.org/10.1007/s10584-011-0152-3, 2011a.

van Vuuren, D. P., Edmonds, J., Kainuma, M., Riahi, K., Thomson, A., Hibbard, K., Hurtt, G. C., Kram, T., Krey, V., Lamarque, J.-F., Masui, T., Meinshausen, M., Nakicenovic, N., Smith, S. J., and Rose, S. K.: The representative concentration pathways: an overview, Climatic Change, 109, 5–31, https://doi.org/10.1007/s10584-011-0148-z, 2011b.

Wang, W., Bruyère, C., Duda, M., Dudhia, J., Gill, D., Kavulich, M., Keene, K., Lin, H.-C., Michalakes, J., Rizvi, S., Zhang, X., Berner, J., and Smith, K.: WRF ARW Version 3 Modeling System User's Guide, 1–428, https://doi.org/10.1525/jps.2007.37.1.204, 2015.

Werner, M., Tegen, I., Harrison, S. P., Kohfeld, K. E., Prentice, I. C., Balkanski, Y., Rodhe, H., and Roelandt, C.: Seasonal and interannual variability of the mineral dust cycle under present and glacial climate conditions, J. Geophys. Res., 107, 4744, https://doi.org/10.1029/2002JD002365, 2002.

Wild, M.: Global dimming and brightening: A review, J. Geophys. Res., 114, D00D16, https://doi.org/10.1029/2008JD011470, 2009.

Woodward, S., Roberts, D. L., and Betts, R. A.: A simulation of the effect of climate change-induced desertification on mineral dust aerosol, Geophys. Res. Lett., 32, L18810, https://doi.org/10.1029/2005GL023482, 2005.

Young, P. J., Arneth, A., Schurgers, G., Zeng, G., and Pyle, J. A.: The $CO_2$ inhibition of terrestrial isoprene emission significantly affects future ozone projections, Atmos. Chem. Phys., 9, 2793–2803, https://doi.org/10.5194/acp-9-2793-2009, 2009.

Young, P. J., Archibald, A. T., Bowman, K. W., Lamarque, J.-F., Naik, V., Stevenson, D. S., Tilmes, S., Voulgarakis, A., Wild, O., Bergmann, D., Cameron-Smith, P., Cionni, I., Collins, W. J., Dalsøren, S. B., Doherty, R. M., Eyring, V., Faluvegi, G., Horowitz, L. W., Josse, B., Lee, Y. H., MacKenzie, I. A., Nagashima, T., Plummer, D. A., Righi, M., Rumbold, S. T., Skeie, R. B., Shindell, D. T., Strode, S. A., Sudo, K., Szopa, S., and Zeng, G.: Preindustrial to end 21st century projections of tropospheric ozone from the Atmospheric Chemistry and Climate Model Intercomparison Project (ACCMIP), Atmos. Chem. Phys., 13, 2063–2090, https://doi.org/10.5194/acp-13-2063-2013, 2013.

Zhang, Q. J., Beekmann, M., Drewnick, F., Freutel, F., Schneider, J., Crippa, M., Prevot, A. S. H., Baltensperger, U., Poulain, L., Wiedensohler, A., Sciare, J., Gros, V., Borbon, A., Colomb, A., Michoud, V., Doussin, J.-F., Denier van der Gon, H. A. C., Haeffelin, M., Dupont, J.-C., Siour, G., Petetin, H., Bessagnet, B., Pandis, S. N., Hodzic, A., Sanchez, O., Honoré, C., and Perrussel, O.: Formation of organic aerosol in the Paris region during the MEGAPOLI summer campaign: evaluation of the volatility-basis-set approach within the CHIMERE model, Atmos. Chem. Phys., 13, 5767–5790, https://doi.org/10.5194/acp-13-5767-2013, 2013.